JNeurosci
THE JOURNAL OF NEUROSCIENCE

Research Articles: Neurobiology of Disease

The glycoside oleandrin reduces glioma growth with direct and indirect effects on tumor cells

Stefano Garofalo[1], Alfonso Grimaldi[1], Giuseppina Chece[1], Alessandra Porzia[2], Stefania Morrone[3], Fabrizio Mainiero[3], Giuseppina D'Alessandro[1,4], Vincenzo Esposito[4,5], Barbara Cortese[6], Silvia Di Angelantonio[1,7], Flavia Trettel[8] and Cristina Limatola[4,8]

[1]*Department of Physiology and Pharmacology, Sapienza University, 00185 Rome Italy*

[2]*Department of Molecular Medicine, Sapienza University, 00185 Rome, Italy*

[3]*Department of Experimental Medicine, Sapienza University, 00185 Rome, Italy*

[4]*IRCCS Neuromed, Via Atinense 18, 86077 Pozzilli, IS, Italy*

[5]*Department of Neurology and Psychiatry, Sapienza University, Piazzale Aldo Moro 5, 00185 Rome Italy*

[6]*Consiglio Nazionale delle Ricerche - Nanotec, Institute of Nanotechnology, Soft and living matter lab, Department of Physics, Sapienza University, 00185, Rome Italy.*

[7]*Center for Life Nanoscience - Istituto Italiano di Tecnologia@Sapienza, Rome Italy*

[8]*Department of Physiology and Pharmacology, Sapienza University, Laboratory affiliated to Istituto Pasteur Italia — Fondazione Cenci Bolognetti, Piazzale Aldo Moro 5,00185 Rome Italy.*

DOI: 10.1523/JNEUROSCI.2296-16.2017

Received: 18 July 2016

Revised: 27 February 2017

Accepted: 27 February 2017

Published: 14 March 2017

Author contributions: S.G., A.P., S.M., F.M., V.E., S.D.A., F.T., and C.L. designed research; S.G., A.G., G.C., A.P., S.M., B.C., and S.D.A. performed research; S.G., A.G., G.C., A.P., S.M., B.C., S.D.A., and C.L. analyzed data; S.G., F.M., B.C., S.D.A., F.T., and C.L. wrote the paper; G.D. contributed unpublished reagents/analytic tools.

The authors declare no competing financial interests. This work was supported by AIRC IG2015-16699 to C.L. and through the grant MFAG n. 16803 to B.C.

Corresponding author: Cristina Limatola, Department of Physiology and Pharmacology, Sapienza University, Piazzale Aldo Moro 5,00185 Rome Italy; email: cristina.limatola@uniroma1.it

Cite as: J. Neurosci ; 10.1523/JNEUROSCI.2296-16.2017

The glycoside oleandrin reduces glioma growth with direct and indirect effects on tumor cells

Abbreviated title: Brain tumor growth is reduced by oleandrin in vivo

Stefano Garofalo[1], Alfonso Grimaldi[1], Giuseppina Chece[1], Alessandra Porzia[2], Stefania Morrone[3], Fabrizio Mainiero[3], Giuseppina D'Alessandro[1,4], Vincenzo Esposito[4,5], Barbara Cortese[6], Silvia Di Angelantonio[1,7], Flavia Trettel[8], Cristina Limatola[4,8]

[1]Department of Physiology and Pharmacology, Sapienza University, 00185 Rome Italy; [2]Department of Molecular Medicine, Sapienza University, 00185 Rome, Italy; [3]Department of Experimental Medicine, Sapienza University, 00185 Rome, Italy; [4]IRCCS Neuromed, Via Atinense 18, 86077 Pozzilli, IS, Italy; [5]Department of Neurology and Psychiatry, Sapienza University, Piazzale Aldo Moro 5, 00185 Rome Italy; [6]Consiglio Nazionale delle Ricerche - Nanotec, Institute of Nanotechnology, Soft and living matter lab, Department of Physics, Sapienza University, 00185, Rome Italy. [7]Center for Life Nanoscience - Istituto Italiano di Tecnologia@Sapienza, Rome Italy; [8]Department of Physiology and Pharmacology, Sapienza University, Laboratory affiliated to Istituto Pasteur Italia – Fondazione Cenci Bolognetti, Piazzale Aldo Moro 5,00185 Rome Italy.

Corresponding author: Cristina Limatola, Department of Physiology and Pharmacology, Sapienza University, Piazzale Aldo Moro 5,00185 Rome Italy; email: cristina.limatola@uniroma1.it

Numbers of pages: 35; Numbers of figures: 10; Number of words for Abstract: 186; Introduction: 628; Discussion: 1113.

Acknowledgements: The authors declare no competing financial interests. This work was supported by AIRC IG2015-16699 to C.L. and through the grant MFAG n. 16803 to B.C.

Abstract

Oleandrin is a glycoside that inhibits the ubiquitous enzyme Na^+-K^+-ATPase. In addition to its known effects on cardiac muscle, recent *in vitro* and *in vivo* evidence highlighted potential for anticancer properties of this compound. In this paper we evaluated for the first time the effect of oleandrin on brain tumors. To this aim mice were transplanted with human or murine glioma and analyzed for tumor progression upon oleandrin treatment. In both systems, oleandrin impaired glioma development, reduced tumor size, and inhibited cell proliferation. We demonstrated that oleandrin i) enhances brain-derived neurotrophic factor (BDNF) level in the brain; ii) reduces both microglia/macrophage (M/Mϕ) infiltration and CD68 immunoreactivity in the tumor mass; iii) decreases astrogliosis in peritumoral area; and iv)reduces glioma cell infiltration in healthy parenchyma. In BDNF deficient mice (bdnftm1Jae/J), and in glioma cells silenced for TrkB receptor expression, oleandrin was not effective, indicating a crucial role for BDNF in oleandrin protective and antitumor functions. In addition, we found that oleandrin increases survival of temozolomide (TMZ) treated mice. Altogether these results encourage the development of oleandrin as possible co-adjuvant agent in clinical trials of glioma treatment.

Significance statement

In this work we paved the road for a new therapeutic approach for the treatment of brain tumor, demonstrating the potential of using the cardioactive glycoside oleandrin as co-adjuvant drug to standard chemotherapeutics such as temozolomide.

In murine models of glioma, we demonstrated that oleandrin significantly increased mice survival and reduced tumor growth, both directly on tumor cells and indirectly by promoting an anti-tumor brain microenvironment with a key protective role played by the neurotrophin BDNF.

Introduction

Glioma is the most diffuse and aggressive neoplasm of the nervous system, characterized by high invasion and proliferation, diffuse apoptosis and necrosis, astrogliosis, and microglia/macrophage (M/Mϕ) infiltration, with a poor prognosis. Despite continuous progress in neurosurgery, its infiltrative behavior precludes complete tumor resection and this is certainly the main reason for the poor clinical outcome in patients (Giese et al., 2003; Preusser et al., 2011). Standard therapy consists of surgery, radio- and chemotherapy with temozolomide (TMZ), a cytotoxic imidazotetrazine leading to the formation of O6 - methylguanine, which mismatches with thymine in following DNA replication cycles thus affecting several cellular functions, such as apoptosis (Hirose et al., 2001), autophagy (Kanzawa et al., 2004), mitotic catastrophe and senescence-like events (Hirose et al., 2001). In spite of these treatments, glioma invariably recurs with limited increase of patient survival (Stupp et al., 2009); it appears evident that new therapeutic approaches are urgently needed to treat this disease.

The cardiac glycosides oleandrin, extracted from *Nerium oleander*, is a potent inhibitor of the Na^+/K^+-ATPase pump (McGrail et al., 1991; Li et al., 2013). It is used for the treatment of different cardiac diseases, as the block of the pump results in the increase of intracellular Na^+, with reduced activity of the Na^+/Ca^{2+} exchanger, and the consequent increase of intracellular $[Ca^{2+}]$ (McConkey et al., 2000; Poindexter et al., 2007). This produces an increase in cardiac muscle contractility and blood pressure (Jager et al., 2001; Rosskopf et al., 1993). In the last few years anti-tumoral effects of oleandrin were also demonstrated. It is the principal active constituent of PBI-05204, a botanical drug currently in clinical trials (phase I) for solid tumors. In particular, oleandrin targets specifically the human tumor cells over-expressing the Na^+/K^+-ATPase α3 isoform, at difference with murine tumor cells that express both α1 and α3 isoforms in a 1:1 ratio (Yang et al., 2009; Raghavendra et al., 2007; Lin et al., 2013). The binding affinity of oleandrin is 100-fold higher for the α3 *vs* α1

subunit (Blanco, 2005; Rajasekaran et al., 2005). The anti-tumor activity of oleandrin involves anti-proliferative and pro-apoptotic effects on cancer cells, reduced AKT phosphorylation (Raghavendra et al., 2007), increased caspase-3 activity (Nasu et al., 2002), and inhibition of the FGF-2 and NF-κB pathways (Hong et al., 2014). Recently, neuroprotective effects of oleandrin have been described in murine models of ischemia and in the oxygen glucose deprivation model *in vitro*; a possible mediator of neuroprotection in these systems is BDNF (Dunn et al., 2011; Van Kanegan et al. 2014). We have recently demonstrated that BDNF reduced the chemotaxis of glioma cells, inhibiting the small G protein RhoA through the truncated TrkB.T1 receptor, and that BDNF infusion induced reduction of tumor size in glioma bearing mice (Garofalo et al., 2015).

Here we investigated for the first time the effect of oleandrin on the progression and development of glioma in mice, and reported that oleandrin reduced tumor size both in murine and human glioma models. By means of different primary and established human glioma cell lines we demonstrated a direct effect both *in vitro* and *in vivo*, as oleandrin reduced tumor size, increasing apoptosis and/or necrosis in tumor mass, and impaired glioma cell proliferation. In addition, we described that oleandrin can modify the tumor microenvironment, by enhancing BDNF level in brain parenchyma, with effects on glioma progression, and reducing M/Mϕ and $CD68^+$ cell infiltration, astrogliosis and glioma invasion. Interestingly, reduction of BDNF expression (in $bdnf^{+/-}$ mice), or silencing TrkB receptors in transplanted glioma cells abolished the effects of oleandrin on tumor size, supporting the hypothesis of a crucial role of the neurotrophin in modulating the anticancer activity of oleandrin.

Moreover, when glioma-bearing mice were co-treated with TMZ and oleandrin, a significant increase of survival time was observed in comparison with TMZ alone.

Materials and methods

Materials

Transwell inserts were from BD Labware (Franklin Lakes, NJ); anti-pFAK (Cat# sc-11765), anti-F4/80 (M-300)(Cat# sc-25839, RRID:AB_2246477), antibodies (Abs) were from Santa Cruz Biotechnology (Santa Cruz, CA); anti-Caspase 3 (Cat# D175, RRID:AB_2069897), anti-GFAP (Cat# NB300-141, RRID:AB_10001722) and anti-5-bromo-2-deoxyuridine (BrdU) (Cat# NB500169, RRID:AB_341913) were from Novus Biological (Littleton, CO, USA); anti-CD68 (Cat# MCA1957T, RRID:AB_322219) was from D Serotec (Oxford, UK); anti-NeuN (Cat# MAB377B, RRID:AB_2298772) was from Merck Millipore (Vimodrone, Milan, Italy); secondary Abs were from DAKO (Milan, Italy); all cell culture media, fetal bovine serum (FBS), goat serum, penicillin G, streptomycin, glutamine, recombinant human EGF, Thermo Script RT-PCR System, secondary Abs and Hoechst (Cat# 33342, RRID:AB_10626776) were from GIBCO Invitrogen (Carlsbad, CA, USA); PCR kit was from New England Biolabs (Ipswich, MA, USA); human Alpha 1 cDNA in pCMV6-XL6 (ATP1A1 Myc-DDK-tagged- NM-00701.6) was from Origene; oleandrin, phalloidin (P5282), TMZ, BrdU, hematoxylin andeosin, Ab anti-actin (Cat# A2066, RRID:AB_476693), Lentiviral Transduction Particles for TrkB silencing and percoll were from Sigma–Aldrich (Milan, Italy); RNeasy Mini Kit from Qiagen (Hilden, Germany); Ab anti-pAKT (Ser473) (Cat# 9271S, RRID:AB_10694411), anti-AKT (Cat# 9272, RRID:AB_329827) were from Cell Signaling (Danvers, MA, USA), CXCL12 and BDNF were from Peprotech (London, UK).

Mice and cell lines

The experiments described in the present work were approved by the Italian Ministry of Health in accordance with the guidelines on the ethical use of animals from the European Community Council Directive of 22 September 2010 (2010/63/EU). We used C57BL/6 (*wt*) and CB17/Icr-Prkdcscid/IcrIcoCrI (SCID) (RRID:IMSR_RBRC02771) mice from Charles River Laboratories,

and B6.129S4-Bdnftm1Jae/J (bdnf$^{+/-}$) (RRID:IMSR_JAX:002266) from Jackson laboratories. We always used male mice, 2-month old.

The GL261 glioma cell line (RRID:CVCL_Y003; kindly provided by Dr. Serena Pellegatta, IRCCS Besta, Milan) was cultured in DMEM supplemented with 20% heat-inactivated FBS, 100 IU/ml penicillin G, 100 µg/ml streptomycin, 2.5 µg/ml amphotericin B, 2 mM glutamine and 1 mM sodium pyruvate. U87MG (RRID:CVCL_0022), A172 (RRID:CVCL_0131), U251 (ATCC, RRID:CVCL_0021), GL15 (RRID:CVCL_5H95; kindly provided by Dr. Emilia Castigli, Perugia University), MZC (kindly provided by Dr. Antonietta Arcella, Neuromed), primary human glioma cells (obtained from patients at Neuromed), primary murine microglia and astrocytes (obtained as in Catalano et al., 2013), primary human astrocytes (Thermo Fisher N7805100) were cultured in DMEM supplemented with 10% FBS. Both *wt* and mutated p53 GBM cells were used, while all the GBM cell lines used had methylated MGMT (http://p53.free.fr/Database/Cancer_cell_lines/Brain_cancer.html; Cimini et al., 2012; Lee et al., 2016; Biggs et al., 2011, Pinheiro et al., 2016). Human GBM samples (some provided by Dr. Antonio Santoro, Sapienza University) were from patients that gave their informed consent to the use of tissues for research purposes. Primary human GBM cells were obtained as previously described (Sciaccaluga et al., 2010). Derivation and culture conditions for human fibroblast-derived induced Pluripotent Stem Cells (iPSCs) are described in (Lenzi et al., 2015). Human iPSC-derived neurons, obtained as described (Hill et al., 2016), were provided by Dr. Alessandro Rosa (Sapienza University of Rome). Normal cerebral tissue derived from the prefrontal cortex of patients died from heart failure (kindly provided by Dr. Eleonora Aronica, with ethics approval of Amsterdam University).

Intracranial injection of glioma

Male C57BL/6, SCID or *bdnf*$^{+/-}$ mice were anesthetized with chloral hydrate (400 mg/kg, i.p.) and placed in a stereotaxic head frame. Animals were stereotactically injected with 7.5x10^4 GL261, 5

147 $x10^4$ U87MG; $5x10^5$ U251 and GBM19, $7.5x10^4$ shRNA-TkB GL261: a median incision of ~1 cm
148 was made, a burr hole was drilled in the skull, and cells were injected 2 mm lateral (right) and 1 mm
149 anterior to the bregma, in the right striatum. Cell suspensions, in PBS (4 µl), were injected with a
150 Hamilton syringe at a rate of 1 µl/min at 3 mm depth. After 17 days, animals were sacrificed for
151 different analyses.
152
153 **Histopathological evaluation of tumor volume**
154 Brains of glioma bearing mice were isolated and fixed in 4% buffered formaldehyde. Coronal brain
155 sections (20 µm) were prepared by standard procedures and stained with hematoxylin and eosin.
156 One section every 100 µm was collected and the tumor area was evaluated using Image Tool 3.00.
157
158 **Ca^{2+} imaging**
159 Fluorescence images were acquired at room temperature (24–25 °C) using a customized digital
160 imaging microscope. Excitation of fluorophores at various wavelengths was achieved using a 1-nm-
161 bandwidth polychromatic light selector (Till Polychrome II), equipped with a 150 W xenon lamp
162 (Till Photonics, Germany). Fluorescence was visualized using an upright microscope (Axioscope 1)
163 equipped with a 40x water-immersion objective (Achroplan Carl Zeiss, USA) and a digital 12 bit
164 CCD camera system (Cool Snap EZ, Photometrics). All the peripheral hardware controls, image
165 acquisition and image processing were achieved using MetaFluor software (Molecular Device,
166 USA). Changes in the intracellular Ca^{2+} level were monitored using the high affinity Ca^{2+} sensitive
167 indicator Fluo4-AM (Invitrogen). Neurons were loaded by incubating coverslips for 45 min at 37°C
168 in 1 mL of HEPES-buffered salt solution (HBSS) containing: 120 mM NaCl, 5.4 mM KCl, 1.8 mM
169 CaCl2, 0.8 mM MgCl2, 20 mM HEPES-NaOH, and 15 mM glucose (pH 7.3), plus 5 mg/ml of
170 bovine serum albumin (BSA) and 5 µM of Fluo4-AM. For time-lapse recordings, Fluo4-AM was

excited at 480 nm (emission filter D535/40 nm, dichroic mirror 505DCLP). Ca^{2+} fluorescence changes are presented as $\Delta F/F_0=(F-F_0)/F_0$, where F is the current fluorescence intensity, F_0 is the fluorescence intensity before drug application.

TrkB silencing by shRNA

GL261 cells were infected by TrkB shRNA lentiviral particles. Cells (1.6×10^4) were plated in 96-well plates and infected for 24 h according to the manufacturer's instructions. Transduced cells were selected with 2 μg/ml puromycin. Knockdown efficiency was evaluated by PCR and invasion experiments. Note that the shRNA used is for all the TrkB isoforms.

Transfection of U87MG cells with ATP1A1 cDNA

U87MG cells were plated and allowed to adhere overnight. ATP1A1 cDNA (1 μg) was transfected with LipofectAMINE 2000 (Invitrogen). Transfection efficiency was evaluated by PCR. Twenty-four hours after transfection, cells were treated with oleandrin and analyzed for viability as described above.

Survival Analysis

After tumor cell injection, mice were daily monitored. The end point was determined by lack of physical activity or death. The mean survival time was calculated using the Kaplan–Meier method, and statistical analysis was performed using a log-rank test. For co-treatment with TMZ, 10 days after tumor injection, mice were treated with oleandrin (0.03, 0.3 or 3 mg/kg/daily i.p.), TMZ (50 mg/kg i.p. every two days for four times with a stop of two weeks) or both. Daily treatment with oleandrin was chosen considering (Ni et al., 2002) the pharmacokinetic analyses performed in mice, where oleandrin has a half life of 0.4 h when given i.v. and of 2.3 h when given p.o. The dosing scheme was chosen starting from these data, so to be reasonably sure that a constant concentration

of drug was maintained along the experiment. Animals used in Kaplan-Meier survival studies received up to four TMZ cycles.

BrdU injection

17 days after injection of GL261 or U87MG cells, BrdU was i.p. injected into mice (50 mg/kg). Two hours later, mice were sacrificed and brains processed for immunostaining.

Immunostaining

17 days after injection of GL261 and U87MG cells, mice were sacrificed, and the brains fixed in 4% formaldehyde and snap frozen. Cryostat sections (10 µm) were washed in PBS, incubated with 3% goat serum in 0.3% Triton X-100 for 1h at RT, and then overnight at 4 °C with specific antibodies in PBS containing 1% goat serum and 0.1% Triton X-100. The sections were stained with the following primary Abs: anti-F4/80 (1:50), anti-CD68 (1:200), anti-CASP3 (1:50), anti-BrdU (1:200) and anti-GFAP (1:1000). After several washes, sections were stained with the fluorophore-conjugated antibody and Hoechst for nuclei visualization and analyzed by fluorescence microscope. For BrdU staining, sections were incubated in 1 N HCl for 15 min, then in 2 N HCl for 25 min at 37 °C and neutralized by incubation in 0.1 M borate buffer. For F4/80 staining, coronal sections were boiled for 10 min in citrate buffer (pH 6.0) at 95-100 °C.

Image acquisition and data analysis

Images were digitized using a CoolSNAP camera (Photometrics) coupled to a ECLIPSE Ti-S microscope (Nikon) and processed using MetaMorph 7.6.5.0 image analysis software (Molecular Device). Brain slices were scanned by consecutive fields of vision (x 10 objective lens) to build a single image per section. The percentage of positive cells was measured as the ratio of the area occupied by fluorescent cells versus the total tumor area (by converting pixel to mm^2). For

comparison between different treatments, at least 12 coronal sections per brain around the point of injection were analyzed.

Isolation of NeuN-positive cells and extraction of total RNA

The brains of GBM bearing C57BL/6 mice were cut in small pieces and single-cell suspension was achieved by enzymatic digestion in trypsin (0.25 mg/ml) solution in Hank's balanced salt solution (HBSS). The tissue was further mechanically dissociated using a wide-tipped glass pipette and the suspension applied to a 70 µm nylon cell strainer. Cells, obtained after a three-step Percoll gradient (Guez-Barber et al., 2012), were stained with anti-NeuN Ab (1:1000) at 4 °C for 30 min and isolated using a BD FACS Aria II (BD Biosciences). Cell purity was verified by flow cytometry and PCR analysis. After cell sorting, total RNA was isolated by RNeasy Mini Kit, and processed for real-time PCR.

Real-time PCR

Contralateral and ipsilateral brain hemispheres of injected mice, or cells, were lysed in Trizol reagent (Invitrogen) for RNA isolation. Real-time PCR (RT-PCR) was carried out in a I-Cycler IQ Multicolor RT-PCR Detection System (Biorad) using SsoFast Eva Green Supermix (Biorad) according to the manufacturer's instructions and the cDNAs were amplified with specific primer pairs: bdnf: 5'-TGAGTCTCCAGGACAGCAAA-3' and 5'-TGTCCGTGGACGTTTACTTCT-3'; mmp9: 5'-TAGCTACCTCGAGGGCTTCC-3' and 5'- GTGGGACACATAGTGGGAGG3'; mmp2: 5'- AGGAATCGGGCCTAAAATTG; 3' and 5'- TGCTTTTCAGTGTTTTGGTGA-3'; gapdh: 5'-TCGCTCCCGTAGACAAAATGG-3' and 5'-TTGAGGTCAATGAAGGGGTC-3'. The PCR protocol consisted of 40 cycles of denaturation at 95 °C for 30 s and annealing/extension at 60 °C for 30 s. For quantification, the comparative Threshold Cycle (Ct) method was used. The Ct values from each gene were normalized to the Ct value of GAPDH in the same RNA samples.

Relative quantification was performed using the $2^{-\Delta\Delta Ct}$ method (Schmittgen and Livak, 2008) and expressed as fold changes in arbitrary values.

Measurement of BDNF by ELISA

The brain of mice bearing gliomas was analyzed for BDNF content using a sandwich ELISA (Promega BDNF E_{MAX} Immuno Assay System), following the manufacturer's instructions.

Cell viability *in vitro*

To assess the viability of cells exposed to different concentrations of oleandrin, murine and human tumors and normal cells ($13 \times 10^4/cm^2$) were treated with oleandrin (0.3, 3 or 30 μM) for 3, 8, 20 and 40 h. Cell viability was determined by MTT assay or by staining dead cells as described (Volontè et al., 1994). Results are expressed as % of cell survival, taking as 100% the cells treated with vehicle.

Western blot analyses

Cells were stimulated with oleandrin (3 μM) and/or CXCL12 (50 ng/ml) and EGF (100 ng/ml) for 1 min. The same amount of proteins (20 or 50 μg/sample) was loaded onto 7.5 or 12% SDS polyacrylamide gel and transferred to nitrocellulose paper at 4 °C for 2 h. Blots were incubated for 1 h with 5% non fat dry milk or 3% BSA in Tris-buffered saline containing 0.2% Tween 20 to block non specific binding sites and then incubated overnight at 4 °C with specific primary Abs. After washing, membranes were incubated with HRP-conjugated secondary Abs, and the immunoreactivity was detected by ECL. Densitometric analysis of immune reactive bands was performed using Chemi-Doc XRS, and Quantity One software (Bio-Rad).

Reverse transcription PCR

Total RNA was isolated from human and murine glioma cells, GBM tissues from patients, microglia, human or murine astrocytes, human neurons derived from iPS cells, or murine NeuN positive cells, using the RNA miniprep. DNA contamination was removed according to the manufacturer's protocol. 500ng of RNA was reverse transcribed using the Thermo Script RT-PCR System protocol and the cDNAs were amplified by PCR with specific primers: for mouse α1, 5'-ATCTGAGCCCAAACACCTGCTAGT-3' and 5'-AAGCGTCCTTCAGCTCTTCATCCA-3'; mouse α3, 5'-AGCCGCCAAGATGGGGGACAAAA-3' and 5'-TGTGTCAGACCCTGCACGCAGTC-3'; human α1, 5'-CTGGCTGGAGGCTGTCATCTTCTTCAT-3' and 5'-GTTGGGGCTCCGATGTGTTGGGGT-3'; human α3, 5'-CTGGCTGGAGGCTGTCATCTTCTTCAT-3' and 5'-ATCGGTTGTCGTTGGGGTCCTCGGT-3'; mouse actin, 5'-GTCACCCACACTGTGCCCAT-3' and 5'-ACAGAGTACTTGCGCTCAGGA-3'; human actin, 5'-TAAGGAGAAGCTGTGCATCG-3' and 5'-GGAGCAATGATCTTGATCTTC-3'; βTubIII, 5'-CGCACGACATCTAGGACTGA-3' and 5'-TGAGGCCTCCTCTCACAAGT-3'; GFAP, 5'-GGCCGGGGCGCTCAA-3' and 5'-GCCGACTCCCGCGCAT-3'; CX3CR1, 5'-TCACGTTCGGTCTGGTGGG-3' and 5'-GGTTCCTAGTGGAGCTAGGG-3'; CX3CL1, 5'-CTTCCTTTCTCCCCGAGGTA-3' and 5'-CCAGGCTGGCTATGGTCCAACTG-3'; human TrkB-FL, 5'-CTTTGGTAATGCTGTTTCTG-3' and 5'-CGCGGCGATCTGCTGGGCTAT-3'; human TrkB-T1, 5' GGGAGGGATGAGAAACAGATTC-3' and 5'-CGGGATAAGCCAACAGCAGTC-3'. The PCR reaction was as follow: DNA was denatured for 2 min at 94 °C and sequences were amplified for 35 cycles for α3 and α1 94 °C for 45 s; 60 °C for 55 s; 72 °C for 90 min; for CX3CR1 and CX3CL1 94 °C for 30 s; 60 °C for 30 s; 72 °C for 2 min; for GFAP, actin, βTubIII, TrkB-FL, TrkB-T1 94 °C 30 s; 57 °C 2 min; 72 °C 40 s, followed by the last extension step at 72 °C for 10 min. A MJ Mini

294 Thermal Cycler (Biorad, Segrate MI, Italy) was used for all the reactions. Products were analyzed
295 on 2% agarose gels stained by ethidium bromide.
296
297 **Boyden Chamber chemotaxis assays**
298 Semi-confluent cells were trypsinized, preincubated in chemotaxis medium (DMEM without
299 glutamine, 100 IU/ml penicillin G, 100 µg/ml streptomycin, 0.1% BSA, and 25 mM HEPES, pH
300 7.4) supplemented with AraC 5 µm, for 15 min, and plated (4 x 10^4 cells) on poly-L-lysine-coated
301 transwells (8 µm pore size filters) in this same medium. The lower chamber contained oleandrin
302 (0.3, 3 or 30 µM), EGF (100 ng/ml), CXCL12 (50 ng/ml) or vehicle. After 4 h (U87MG, U251,
303 MZC, GL15, A172, GBM19 and GBM46) or 18 h (GL261), cells were fixed with trichloroacetic
304 acid. Cells adhering to the upper side of the filter were scraped off, and cells on the lower side were
305 stained with a solution containing 50% isopropanol, 1% formic acid, and 0.5% (wt/vol) brilliant
306 blue R 250. For each membrane, the stained cells were counted in at least 20 fields with a 40x
307 objective. Experiments were done in six repeats and performed four times.
308
309 **Apoptosis assay**
310 Cells (3.5 x10^4) were seeded into 12-well plates (in triplicates) and, after 24 h, treated with
311 oleandrin (3 µM) for 10 h. To detect apoptosis, cells were harvested, washed (with buffer
312 containing 10 mM HEPES, 140 mM NaCl, and 2.5 mM $CaCl_2$), and re-suspended in FITC-
313 conjugated Annexin V (Bender MedSystems, Austria). After 15 min of incubation at RT, propidium
314 iodide (PI) was added, and the percentage of AnnexinV-FITC and Annexin V-FITC/PI positive
315 cells was determined.
316
317 **Statistical data analysis**

318 Data are shown as the mean ± s.e.m.. Statistical significance was assessed by Student's t-test or one-
319 way ANOVA for parametrical data, as indicated; Holm-Sidak, test was used as post-hoc test;
320 Kruskas-Wallis, for non-parametrical data, followed by Dunn or Tukey post hoc tests. For multiple
321 comparisons, multiplicity-adjusted p values are indicated on the respective figures; the p values are
322 indicated by * $p < 0.05$, ** $p < 0.01$. For statistical analysis of calcium responses in different glioma
323 cell types at different drug concentrations, statistical difference of proportions was obtained with
324 Chi-square or z-test. For the Kaplan–Meier analysis of survival, log-rank test was used. All
325 statistical analyses were done using Sigma Plot 11.0 software.
326

Results

Oleandrin differentially affects intracellular Ca^{2+} in human and murine glioma cells

Prior to investigating the effect of oleandrin on glioma growth, we analyzed the expression of the Na^+/K^+-ATPase subunits α1and α3, known molecular targets of this drug, in different human cell lines of GBM, in cells from GBM patients, and in murine glioma cells. We also analyzed the Na^+/K^+-ATPase subunit expression in human normal astrocytes and neurons derived from iPSCs and in murine astrocytes, microglia and neurons. Data shown in Fig. 1a,b demonstrated that all the GBM and glioma cell lines, and primary cells from patients, express both the α1 and α3 subunits, with different ratio, that is higher for human cells (1:2.5 for U87MG and for 1:11.5 for GBM19) in respect to murine GL261 (1:1, n=3, ** $p<0.01$). We also confirmed that neuronal cells express high levels of α3, whilst normal glia (astrocytes and microglia) have higher levels of the α1 subunit (Fig. 1b).

To understand whether such different expression resulted in different functional effects of oleandrin in cells of distinct origins, considering the higher affinity for α3 subunit (Blanco et al, 2005), we measured intracellular Ca^{2+} transients upon drug treatment. It is known that blockade of the Na^+/K^+ ATPase affects Ca^{2+} homeostasis, leading to increase of intracellular of Ca^{2+} concentrations $[Ca^{2+}]_i$ (McConkey et al., 2000). We performed intracellular Ca^{2+} measurements loading cells with the Fluo4-AM dye. Data obtained indicate that oleandrin (1 μM) induces a transient increase of $[Ca^{2+}]_i$ in human (U87MG) cells (Fig 1c). The number of responsive U87MG cells (Fig. 1d) and the level of $[Ca^{2+}]_i$ (Fig. 1e) increased with oleandrin dose (n= 44/78; 98/118/; 115/123 cells, at 1, 3 and 30 μM respectively. *$p<0.05$ among 1 μM and the other doses). In contrast, murine GL261 cells showed a remarkably different profile of Ca^{2+} response, with a small proportion of responsive cells only at 30 μM oleandrin (23/134 cells) (Fig. 1d).

Altogether, these results demonstrate that human glioma cells display higher expression ratio of the α3/α1 subunits than murine cells and, consistently, only human (U87MG) cells responded to oleandrin in term of intracellular Ca^{2+} transients.

Oleandrin induces apoptosis and reduces migration of human glioma cells *in vitro*

To investigate the effects of oleandrin in glioma, cell viability and migration were examined. Data shown in Fig. 2a describe that oleandrin reduced viability in all human GBM cells, in a time dependent way, already at the lowest dose (n=4, ** $p<0.01$), whilst no effect on viability was observed in GL261 cells (Fig. 2a). To verify the hypothesis that the different effects on human and murine cells were due to the different expression ratio of the Na+/K+ ATPase α1: α3 subunits, we overexpressed α1 in U87MG cells. Data shown in Fig. 2b,c demonstrate that such manipulation, switching the α1: α3 ratio to 1:1.1, renders U87MG cell growth insensitive to oleandrin, even at higher dose. We then tested the apoptosis of glioma cells exposed to oleandrin (3 μM for 10 h) by flow cytometry. Oleandrin treatment resulted in a significant increase of apoptotic frequency in U87MG cells (n=6, ** $p<0.01$), with no variation in GL261 cells (Fig. 2d). To evaluate the specific effect of oleandrin on tumor cells, we investigated the viability of normal human and murine cerebral cells. At this aim the effect of oleandrin was tested at doses from 0.3 to 30 μM, on normal human astrocytes and human iPSC-derived neurons, as well as on primary cultures of murine astrocytes, neurons or microglia. The viability of these cells was not affected by oleandrin (data not shown); only for microglia, we observed a reduction of cell viability using 30 μM oleandrin (at 40 h, 70.7 ± 4.1%, vs C; n=3 *$p<0.05$, one –way ANOVA followed by Holm Sidak post hoc test).

It is known that cell migration is an important aspect of tumor cell infiltration in brain parenchyma (Miao et al., 2015). The Na^+/K^+ pump is involved in modulating the activity of ion channels involved in cell migration, like BK (Tajima et al., 2011), and it is also reported to modulate cell

374 migration independently of its pump activity (Barwe et al., 2005; Balasubramaniam et al., 2015).
375 We evaluated the effect of oleandrin on tumor cell migration: functional assays demonstrated that
376 the migration of human GBM cells toward EGF and CXCL12 was reduced by oleandrin in a dose
377 dependent way (n=4-5, *p<0.05, ** p<0.01), whilst GL261 migration was not affected (Fig. 2e).
378 Interestingly, oleandrin also reduced CXCL12- and EGF induced AKT and FAK phosphorylation in
379 U87MG but not in GL261 cells (n=4-5, *p<0.05, ** p<0.01), as demonstrated by western blot and
380 immunofluorescence analyses (Fig. 3a-c), in accordance with the specific functional effects on these
381 cells. These results confirm a direct effect of oleandrin on human tumor cells. In line with these
382 results, oleandrin treatment also reduced the chemoattractant-induced increase of metalloproteinases
383 (MMPs) 2 and 9, thus confirming a wide spectrum effect on tumor cell migration (Fig. 3d, n=4,
384 **p<0.01).
385
386 **Oleandrin affects tumor growth in mice**
387 We investigated the effect of oleandrin on glioma growth *in vivo*. To this aim, SCID or C57BL/6
388 mice were transplanted, respectively, with human U87MG ($5x10^4$), U251, GBM19 ($5x10^5$) or
389 murine (syngeneic) GL261 ($7.5x10^4$) cells into the right striatum and, after 10 days, treated daily
390 with oleandrin (i.p.) for additional 7 days (Fig. 4a). Fig. 4b,c (left) show that oleandrin significantly
391 reduced tumor sizes in human and murine glioma cell models *in vivo*, in a dose-dependent way.
392 High concentrations of oleandrin (3 mg/kg) were fatal in both models, as expected from the known
393 lethal dose for rodents (Kumar et al., 2013). Doses of oleandrin below the lethal dose (0.3 mg/kg)
394 significantly increased the survival time from 32.6 ± 1.4 days to 53.8 ± 9.6 days in mice injected
395 with U87MG cells (** p<0.01 log rank test, n=5-11), and from 23.37 ± 1.2 days to 34.38 ± 3.3 days
396 (** p<0.01 log rank test, n=5-11, Fig. 4b, right) in mice injected with GL261 cells (Fig. 4c right).
397 Reductions of tumor volumes were obtained also when different human GBM cells were injected

(Fig. 4d,e; U251, C: 0.34 ± 00.8 mm^3, oleandrin (Ole): 0.07 ± 0.01 mm^3 ** $p<0.01$ n= 5 and GBM19, C: 22.6 ± 4.7 mm^3, Ole: 4.9 ± 2.3 mm^3 * $p<0.05$ n= 5).

Oleandrin reduces glioma cell proliferation and induces death of glioma cells *in vivo*

To investigate the mechanisms by which oleandrin can reduce glioma size *in vivo*, we analyzed the extent of tumor cell proliferation and death in the brain of glioma bearing mice. Results reported in Fig. 5a,b demonstrate that oleandrin significantly reduced the extent of 5-bromo-2-deoxyuridine (BrdU) positive cells (evaluated as described in Methods), and increased the percentage of cleaved caspase 3 positive cells in U87MG tumor mass (** $p<0.01$ * $p<0.05$; n=4-8 mice). Differently, in mice bearing GL261 tumors, oleandrin treatment caused a reduction of BrdU positive cells, with no variations in the cleaved caspase 3 level (Fig. 5c,d). These results suggest that the effect of oleandrin on tumor size could be mediated through induction of apoptosis and reduction of tumor cell proliferation in human glioma, whilst in murine cells the reduction of tumor growth is not dependent on the activation of apoptotic pathways.

Oleandrin reduces glia reactivity and tumor invasiveness.

We analyzed the effect of oleandrin treatment on brain parenchyma of both mouse models, looking at M/Mϕ infiltration (evaluated as $F4/80^+$ cells) and activation of phagocytic activity ($CD68^+$ cells) within the tumor, and astrocyte activation at tumor border (glial fibrillary acidic protein, $GFAP^+$ cells). Data shown in Fig. 6a-c demonstrated a significant reduction of $F4/80^+$ cell infiltration in the tumor mass, as well as a reduction of $CD68^+$ and double positive F4/80/CD68 cells, within the tumor (** $p<0.01$ * $p<0.05$ n=4 mice). Moreover, astrogliosis, a common feature typically observed in peritumoral area, was significantly reduced by oleandrin, as indicated by the decreased GFAP staining at the tumor border (* $p<0.05$, n=4 mice) (Fig. 6d).

The effect of oleandrin on the invasion of brain parenchyma by tumor cells was investigated in cerebral slices of mice injected with human and mice glioma. In GL261 injected mice, we observed a reduced number of glioma cells protruding from the main tumor mass (n=5 mice per condition; ** $p<0.01$) (Fig. 6e), indicative of a reduced tendency of tumor cells to migrate and invade the surrounding tissue. This inhibitory effect was also observed in human U251- and GBM19-, but not in U87MG-injected mice where, also in the control condition, glioma cells did not invade brain parenchyma (n=3 mice) (Fig. 6e). Unlike the other cell lines used in this study, in fact, U87MG is not invasive in mouse brain parenchyma.

Oleandrin enhances BDNF level in the brain

Data reported above demonstrate that, *in vivo*, oleandrin can affect the growth of human and mouse glioma. However, all our *in vitro* experiments indicate that oleandrin has no direct effects on murine glioma cells. To understand which mechanism could mediate the effect of oleandrin on the growth of murine glioma *in vivo*, we investigated brain BDNF expression and production upon oleandrin treatment (Dunn et al, 2011). We observed that oleandrin (0.3 mg/kg) increased BDNF mRNA level in the brain of GL261 glioma bearing mice, measured 3 days after oleandrin administration (drug administration starting 10 days after glioma inoculation), and such increase was still present after 7 days (n=5-4, * $p<0.05$, ** $p<0.01$, Fig. 7a); comparable results were obtained measuring protein BDNF levels (n=5-4, * $p<0.05$, ** $p<0.01$, Fig. 7b). A similar increase of BDNF mRNA and proteins was observed in the brain of SCID mice injected with U87MG cells (n=5-4, * $p<0.05$, ** $p<0.01$, Fig 7c,d).

To understand which cells produce BDNF upon oleandrin treatment, we focused our attention on neurons, the only cell type that in the brain expresses the $\alpha 3$ subunit of the Na^+/K^+-ATPase (Cahoy et al., 2008). Cells from the brain of mice transplanted with GL261 were sorted for NeuN expression by FACS and analyzed for BDNF expression. The efficacy of cell sorting was verified

by PCR, showing that sorted cells were positive βTubIII and CX3CL1 and negative for CX3CR1 and GFAP (not shown). Quantitative PCR analyses revealed that the $NeuN^+$ cells showed increased BDNF expression upon oleandrin treatment (0.3 mg/kg) (n=5, * $p<0.05$, ** $p<0.01$, Fig. 7e) thus revealing an effect of oleandrin on neuronal cells. To verify a direct effect of oleandrin on neurons, calcium imaging experiments were performed on cortical neurons in culture; data reported in Fig. 7f show that acute oleandrin (3 μM) application induced fast and reversible intracellular Ca^{2+} rise in 15/57 neurons (** $p<0.01$).

To confirm the hypothesis that BDNF could be an important mediator of oleandrin effect on glioma, we transplanted *bdnf*$^{+/-}$ mice with GL261 cells and treated them with oleandrin as described above. Control experiments confirmed that oleandrin did not increase BDNF production in the brain of these mice (data not shown). At 17 days after glioma injection, mice were sacrificed and brains analyzed for tumor volumes. Data shown in Fig. 7g indicate that *bdnf*$^{+/-}$ mice developed larger tumors in comparison with their *wt* littermates, and that in these mice oleandrin was ineffective in reducing tumor size (n=5, * $p<0.05$).

To further investigate the involvement of TrkB, we silenced TrkB by shRNA in GL261 cells, injected silenced cells in mouse brains and treated the animals with oleandrin, as previously described, and analyzed tumor volumes after 17 days. Data reported in Fig. 7g (n=5), demonstrated that oleandrin is not effective in reducing tumor volumes in these mice, thus confirming that BDNF mediates the indirect effect of oleandrin on tumor cells.

TrkB receptor expression and function were investigated using both the cell lines adopted here and in normal human brain tissue, as control. Fig. 8 demonstrates that the human GBM cells used here only express the truncated TrkB.T1, and that BDNF stimulation of these cells reduced the migration induced by EGF (n=5, **$p<0.01$), confirming previous data on murine glioma (Garofalo et al., 2015).

Oleandrin and TMZ co-treatment increases the survival of GL261-bearing mice

The first line chemotherapic drug currently used to treat glioma patients is the alkylating agent TMZ. We investigated the effect of oleandrin/TMZ co-treatment in term of mouse survival. Mice injected with GL261 cells were treated with the drugs, alone or in combination (as described in Methods). Our results (Fig. 9) demonstrated that the co-treatment (oleandrin/TMZ) significantly prolonged mice survival with respect to single treatments (Vehicle: 23.8 ± 0.9 days n=11; Ole: 40.5 ± 6.5 days n=11; TMZ: 43.2 ± 7.5 days n=9; Ole + TMZ: 67.6 ± 10.5 days n=9; ** $p<0.01$ vs C; ## $p<0.01$ vs TMZ and Ole; log rank test). These results highlighted the potential for therapeutic use of oleandrin in glioma, also in association with TMZ.

Discussion

Glioblastoma is the most frequent malignant brain tumor, with poor therapeutic perspectives for patients. Oleandrin, in the form of a Nerium oleander extract (PBI-05204), has been used as a novel drug to treat solid tumors due to its ability to kill tumor cells selectively (Manna et al., 2007), and the first phase I clinical trials defined a safe dose for administration to patients (0.2255 mg/kg, Hong et al., 2014). Oleandrin is reported to be cytotoxic to several human tumor cells, like melanoma, prostate tumor, non small cell lung cancer cells, osteosarcoma. In these cells it induces cell apoptosis with different mechanisms involving the activation of NF-κB and caspase, the upregulation of death receptor 4 and 5, and suppression of the Wnt/β catenin signaling pathway (Ma et al., 2015; Pan et al., 2015).

We have investigated for the first time the potential anti-tumor activity of oleandrin in glioma, and found that this botanic drug reduced tumor growth in mice *via* direct and indirect effects on tumor cells. The direct effect of oleandrin is specific for human tumor cells, and consists of apoptosis induction. The indirect effect is mediated by brain parenchyma, where oleandrin stimulated the production and release of the neurotrophin BDNF by neuronal cells. This neurotrophin has a key role in contrasting glioma growth, as demonstrated by the lack of effect of oleandrin in *bdnf*$^{+/-}$ mice and in mice injected with glioma cells silenced for TrkB expression by shRNA. We have also showed that oleandrin reduces microglia/macrophage infiltration and astrocyte activation, and contrasts tumor cell infiltration in the healthy parenchyma.

The direct effect of oleandrin on human tumor cells relies on the higher expression of α3 vs α1 subunit (with respect to mouse glioma cells) of the Na^+/K^+ ATPase pump and is in accordance with the preferential activity of olendrin on α3 subunit (Blanco et al., 2005). Indeed, the α3 subunit is highly expressed by other human tumor cells, and targeting its activity with oleandrin impairs cell growth of several human tumors (Raghavendra et al., 2007). This is further confirmed in our

507 experiments where we abolished the effect of oleandrin on cell viability by changing the α1:α3
508 ratio via overexpression the α1 subunit in U87MG cells. It is important to note that oleandrin does
509 not affect the viability of normal neurons and astrocytes, and has minor effects (at high
510 concentration only) on microglia viability. This would confirm good specificity for tumor cells also
511 in the brain of patients with GBM; however, before considering using oleandrin in humans, it
512 should be taken into account that at high doses (0.3383 mg/kg/day) oleandrin could induce adverse
513 effects like proteinuria, fatigue, nausea, diarrhea and important cardiac alterations (Hong et al.,
514 2014).
515 The efficacy of directly targeting the Na+/K+ ATPase pump for glioma treatment is in line with
516 what was previously shown for another cardiac glycoside, proscillardin A, that specifically targets
517 the α1 subunit on tumor cells, inducing reduced cell growth and apoptosis (Denicolai et al., 2014).
518 Although the α1 subunit is ubiquitously expressed in all brain parenchymal cells (McGrail et al.,
519 1991), in their study authors only considered the direct effect on tumor cells. However, the ability
520 of oleandrin to reduce tumor size and improve mice survival in animals implanted with mouse
521 GL261 cells, bearing low level of α3 subunit, points out to an effect of oleandrin on other cells in
522 brain parenchyma.
523 In line with this, we demonstrated that the indirect effect of oleandrin is mediated by the increased
524 expression of the brain neurotrophin BDNF in glioma bearing mice. An upregulation of *bdnf*
525 expression due to oleandrin has been already shown *in vitro* and correlated to the neuroprotective
526 effect of the botanic drug, PBI-05204, *in vitro* model of ischemia (Van Kanegan et al, 2014).
527 Here we show for the first time that oleandrin induced *bdnf* gene expression and protein production
528 by neuronal cells, consistent with their specific expression of the α3 subunit among the brain
529 parenchymal cells. The mechanism linking Na^+/K^+ ATPase activity to gene expression could
530 involve Ca^{2+} transients generated by the secondary regulation of the Na^+/Ca^{2+} exchanger, via local

alteration of the transmembrane Na^+ gradient, as shown for cardiomyocytes and transformed cells (Rose and Valdes, 1994; Poindexter et al., 2007). Consistently, we demonstrated that in primary neurons in culture, oleandrin induced intracellular Ca^{2+} transients, in a dose dependent way. The oleandrin induced Ca^{2+} transient could mediate *bdnf* promoter activity (Lyons and West, 2011) in neurons, with BDNF production. The role of BDNF in counteracting tumor progression might be due to a direct activity on glioma cells, where it reduces their invasion ability (Garofalo et al., 2015 and this paper), but also to a protective effect on surrounding neurons, that are normally damaged by the increased levels of extracellular glutamate released by tumor cells (Ye and Sontheimer 1999; Mattson et al., 1995). We also show that oleandrin reduced the number and modulated the activation state of tumor infiltrating microglia/macrophage cells, an event correlated with disease severity (Hambardzumyan et al., 2016), and reduced astrocyte activation at the tumor border. These effects resemble those induced by BDNF administration in glioma bearing mice (Garofalo et al., 2015). Accordingly, we demonstrate that BDNF plays a crucial role in the effect of oleandrin, since, in $bdnf^{+/-}$ mice, it failed to increase BDNF expression and was ineffective in reducing tumor volume. BDNF acts on TrkB receptors (mainly TrkB.T1 isoform) expressed on glioma cells, as demonstrated by the inability of oleandrin to reduce tumor volume in mice transplanted with TrkB silenced glioma cells. Our results demonstrate that oleandrin is a drug that can counteract glioblastoma, targeting both tumor cells and the brain microenvironment. The first line chemotherapic drug currently used to treat glioblastoma patients is TMZ (Hirose et al., 2001); here we showed that co-treatment of glioma bearing mice with TMZ and oleandrin strongly prolongs mice survival compared to TMZ treatment alone. In the light of the direct and indirect (BDNF mediated) mechanisms induced by oleandrin on tumor cells, we speculate that this drug might also drive positive effects on GBM with un-methylated or hypo-methylated MGMT promoter. In addition, since standard treatment for GBM patients is TMZ and adjuvant radiotherapy, it would be important to investigate, in future experiments, the effect of oleandrin in irradiated mice.

Altogether, these novel results describe the molecular and cellular mechanisms involved in the activity of oleandrin in tumor-bearing mice, as shown in the scheme of Fig. 10. These data demonstrate the increased efficacy of simultaneously targeting glioma cell proliferation, migration, and the tumor microenvironment in order to counteract glioma progression and pave the road for future clinical trials to test the effect of oleandrin and BDNF as co-adjuvant to TMZ in humans suffering from malignant glioma.

564

565 **REFERENCES**

566 Balasubramaniam SL, Gopalakrishnapillai A, Barwe SP (2015) Ion dependence of Na-K-
567 ATPase-mediated epithelial cell adhesion and migration. Am J Physiol Cell Physiol.
568 309(6):C437-41.

569 Barwe SP, Anilkumar G, Moon SY, Zheng Y, Whitelegge JP, Rajasekaran SA, Rajasekaran
570 AK (2005) Novel role for Na,K-ATPase in phosphatidylinositol 3-kinase signaling
571 and suppression of cell motility. Mol Biol Cell. 16(3):1082-94.

572 Biggs T, Foreman J, Sundstrom L, Regenass U, Lehembre F. J Biomol Screen. (2011)
573 Antitumor compound testing in glioblastoma organotypic brain
574 cultures.Sep;16(8):805-17.

575 Blanco G (2005) Na,K-ATPase subunit heterogeneity as a mechanism for tissue-specific ion
576 regulation. Semin Nephrol. 25(5):292-303.

577 Cahoy JD, Emery B, Kaushal A, Foo LC, Zamanian JL, Christopherson KS, Xing Y,
578 Lubischer JL, Krieg PA, Krupenko SA, Thompson WJ, Barres BA (2008) A
579 transcriptome database for astrocytes, neurons, and oligodendrocytes: a new resource
580 for understanding brain development and function. J Neurosci. 28(1):264-78.

581 Catalano M, Lauro C, Cipriani R, Chece G, Ponzetta A, Di Angelantonio S, Ragozzino D,
582 Limatola C. (2013) CX3CL1 protects neurons against excitotoxicity enhancing GLT-1
583 activity on astrocytes. J Neuroimmunol. 263(1-2):75-82.

584 Cimini A, Mei S, Benedetti E, Laurenti G, Koutris I, Cinque B, Cifone MG, Galzio R, Pitari
585 G, Di Leandro L, Giansanti F, Lombardi A, Fabbrini MS, Ippoliti R. Distinct cellular
586 responses induced by saporin and a transferrin-saporin conjugate in two different
587 human glioblastoma cell lines. (2012) J Cell Physiol 227(3):939-51

588 Denicolaï E, Baeza-Kallee N, Tchoghandjian A, Carré M, Colin C, Jiglaire CJ, Mercurio S,
589 Beclin C, Figarella-Branger D (2014) Proscillaridin A is cytotoxic for glioblastoma
590 cell lines and controls tumor xenograft growth in vivo. Oncotarget 5(21):10934-48.
591 Dunn DE, He DN, Yang P, Johansen M, Newman RA, Lo DC (2011) In vitro and in vivo
592 neuroprotective activity of the cardiac glycoside oleandrin from Nerium oleander in
593 brain slice-based stroke models. J. Neurochem 119: 805-814.
594 Garofalo S, D'Alessandro G, Chece G, Brau F, Maggi L, Rosa A, Porzia A, Mainiero F,
595 Esposito V, Lauro C, Benigni G, Bernardini G, Santoni A, Limatola C (2015)
596 Enriched environment reduces glioma growth through immune and non-immune
597 mechanisms in mice. Nature Comm. 6:6623.
598 Giese A, Bjerkvig R, Berens ME, Westphal M (2003) Cost of migration: invasion of
599 malignant glioma and implications for treatment. J Clin Oncol 21(8):1624-36.
600 Guez-Barber D, Fanous S, Harvey BK, Zhang Y, Lehrmann E, Becker KG, Picciotto MR,
601 Hope BT (2012) FACS purification of immunolabeled cell types from adult rat brain. J
602 Neurosci Methods. 203(1):10-8.
603 Hambardzumyan D, Gutmann H & Kettenmann H (2016) The role of microglia and
604 macrophages in glioma maintenance and progression. Nat. Neurosci 19:20-27.
605 Hill SJ, Mordes DA, Cameron LA, Neuberg DS, Landini S, Eggan K, Livingston DM (2016)
606 Two familial ALS proteins function in prevention/repair of transcription-associated
607 DNA damage. Proc Natl Acad Sci U S A. 113(48):E7701-E7709.
608 Hirose Y, Berger MS, Pieper RO (2001) p53 effects both the duration of G2/M arrest and the
609 fate of temozolomidetreated human glioblastoma cells. Cancer Res. 61:1957–1963.
610 Hong DS, Henary H, Falchook GS, Naing A, Moulder S, Wheler JJ, Tsimberidou A, Durand
611 JB, Khan R, Yang P, Johansen M, Newman RA, Kurzock R (2014) First-in-human

study of pbi-05204, an oleander-derived inhibitor of akt, fgf-2, nf-κB and p70s6k, in patients with advanced solid tumors. Invest New Drugs 32:1204–1212.

Jager H, Wozniak G, Akinturk IH, Hehrlein FW, Scheiner-Bobis G (2001) Expression of sodium pump isoforms and other sodium or calcium ion transporters in the heart of hypertensive patients. Biochim Biophys Acta 1513:149-159.

Kanzawa T, Germano IM, Komata T, Ito H, Kondo Y, Kondo S (2004) Role of autophagy in temozolomide-induced cytotoxicity for malignant glioma cells. Cell Death Differ 11:448–457.

Lee SY (2016) Temozolomide resistance in glioblastoma multiforme. Genes Dis. 3, 198–210

Lenzi J, De Santis R, de Turris V, Morlando M, Laneve P, Calvo A, Caliendo V, Chiò A, Rosa A, Bozzoni I (2015) ALS mutant FUS proteins are recruited into stress granules in induced pluripotent stem cell-derived motoneurons. Dis Model Mech. 8:755-766.

Li B, Hertz L, Peng L (2013) Cell-Specific mRNA Alterations in Na+, K+-ATPase a and b Isoforms and FXYD in Mice Treated Chronically with Carbamazepine, an Anti-Bipolar Drug. Neurochem Res 38:834–841.

Lin Y, Dubinsky WP, Ho DH, Felix E, Newman RA (2008) Determinants of human and mouse melanoma cell sensitivities to oleandrin. J Exp Ther Oncol. 7(3):195-205.

Lyons MR, West AE (2011) Mechanisms of specificity in neuronal activity-regulated gene transcription. Prog Neurobiol 94(3):259-95.

Ma Y, Zhu B, Liu X, Yu H, Yong L, Liu X, Shao J, Liu Z (2015) Inhibition of oleandrin on the proliferation show and invasion of osteosarcoma cells in vitro by suppressing Wnt/β-catenin signaling pathway. J Exp Clin Cancer Res. 34:115.

McGrail KM, Phillips JM, Sweadner KJ. Immunofluorescent localization of three Na, K-ATPase isozymes in the rat central nervous system: both neurons and glia can express more than one Na, K-ATPase. J Neurosci. 1991; 11:381–391.

637 Manna SK, Sah NK, Newman RA, Cisneros A, Aggarwal BB (2000) Oleandrin suppresses
638 activation of nuclear transcription factor- kB, activator protein-1 and c-Jun NH2-
639 terminal kinase. Cancer Res 60: 3838–3847.
640 Mattson MP, Lovell MA, Furukawa K, Markesbery WR (1995) Neurotrophic factors
641 attenuate glutamate-induced accumulation of peroxides, elevation of intracellular
642 Ca2+ concentration, and neurotoxicity and increase antioxidant enzyme activities in
643 hippocampal neurons. J Neurochem. 65(4):1740-51.
644 McConkey DJ, Lin Y, Nutt LK, Ozel HZ, Newman RA (2000) Cardiac Glycosides Stimulate
645 Ca21 Increases and Apoptosis in Androgen independent, Metastatic Human Prostate
646 Adenocarcinoma Cells Cancer Res 60:3807-3812.
647 McGrail KM, Phillips JM, Sweadner KJ (1991) Immunofluorescent localization of three
648 Na,K-ATPase isozymes in the rat central nervous system: both neurons and glia can
649 express more than one Na,K-ATPase. J Neurosci. 11(2):381-91.
650 Miao H, Gale NW, Guo H, Qian J, Petty A, Kaspar J, Murphy AJ, Valenzuela DM,
651 Yancopoulos G, Hambardzumyan D, Lathia JD, Rich JN, Lee J, Wang B (2015)
652 EphA2 promotes infiltrative invasion of glioma stem cells in vivo through cross-talk
653 with Akt and regulates stem cell properties. Oncogene 34(5):558-67.
654 Nasu S, Milas L, Kawabe S, Raju U, Newman RA (2002) Enhancement of radiotherapy by
655 oleandrin is a caspase-3 dependent process. Cancer Letters 185: 145–151.
656 Ni D, Madden TL, Johansen M, Felix E, Ho DH, Newman RA. (2002) Murine
657 pharmacokinetics and metabolism of oleandrin, a cytotoxic component of Nerium
658 oleander. J Exp Ther Oncol. 2(5):278-85.
659 Pan Y, Rhea P, Tan L, Cartwright C, Lee HJ, Ravoori MK, Addington C, Gagea M, Kundra
660 V, Kim SJ, Newman RA, Yang P (2015) PBI-05204, a supercritical CO_2 extract of

661 Nerium oleander, inhibits growth of human pancreatic cancer via targeting the
662 PI3K/mTOR pathway. Invest New Drugs. 33(2):271-9.
663 Pinheiro R, Braga C, Santos G, Bronze MR, Perry MJ, Moreira R, Brites D, Falcão AS.
664 (2016) Targeting Gliomas: Can a New Alkylating Hybrid Compound Make a
665 Difference? ACM Chem Neurosci DOI: 10.1021/acschemneuro.6b00169
666 Poindexter BJ, Feng W, Dasgupta A, Bick RJ (2007) Oleandrin Produces Changes in
667 Intracellular Calcium Levels in Isolated Cardiomyocytes: A Real-Time Fluorescence
668 Imaging Study Comparing Adult to Neonatal Cardiomyocytes. J. Tox. Environ. Health
669 70(6):568-574.
670 Preusser M, de Ribaupierre S, Wöhrer A, Erridge SC, Hegi M, Weller M, Stupp R. (2011)
671 Current concepts and management of glioblastoma. Ann Neurol. 70(1):9-21.
672 Raghavendra PB, Sreenivasan Y, Manna SK (2007) Oleandrin induces apoptosis in human,
673 but not in murine cells: Dephosphorylation of Akt, expression of FasL, and alteration
674 of membrane fluidity Mol Immunol 44: 2292–2302.
675 Rajasekaran SA, Barwe SP, Rajasekaran AK (2005) Multiple functions of Na,K-ATPase in
676 epithelial cells. Semin Nephrol. 25(5):328-34.
677 Rose AM, Valdes R Jr (1994) Understanding the sodium pump and its relevance to disease.
678 Clin Chem. 40(9):1674-85.
679 Rosskopf D, Düsing R, Siffert W (1993) Membrane sodium-proton exchange and primary
680 hypertension. Hypertension. 21(5):607-17.
681 Schmittgen, T. D. & Livak, K. J. (2008) Analyzing real-time PCR data by the comparative
682 C(T) method. Nat. Prot. 3, 1101–1108.
683 Sciaccaluga M, Fioretti B, Catacuzzeno L, Pagani F, Bertollini C, Rosito M, Catalano M,
684 D'Alessandro G, Santoro A, Cantore G, Ragozzino D, Castigli E,Franciolini F et al.

CXCL12 induced glioblastoma cell migration requires intermediate conductance Ca^{2+}-activated K^+ channel activity. Am J Physiol Cell Physiol. 2010; 299: C175–C184.

Stupp R, Hegi ME, Mason WP, van den Bent MJ, Taphoorn MJ, Janzer RC, Ludwin SK, Allgeier A, Fisher B, Belanger K, Hau P, Brandes AA, Gijtenbeek J, et al. (2009) Effects of radiotherapy with concomitant and adjuvant temozolomide versus radiotherapy alone on survival in glioblastoma in a randomised phase III study: 5-year analysis of the EORTCNCIC trial. Lancet Oncol. 10:459-466.

Tajima N, Itokazu Y, Korpi ER, Somerharju P, Käkelä R (2011) Activity of BK(Ca) channel is modulated by membrane cholesterol content and association withNa+/K+-ATPase in human melanoma IGR39 cells. J Biol Chem. 286(7):5624-38.

Uutela M, Lindholm J, Louhivuori V, Wei H, Louhivuori M, Petrovaara A, Kerman KA,Castre E, Castre ML (2012) Reduction of BDNF expression in Fmr1 knockout mice worsens cognitive deficits but improves hyperactivity and sensorimotor deficits. Genes, Brain and Behavior 11: 513–523.

Van Kanegan MJ, He DN, Dunn DE, Yang P, Newman RA, West AE, Lo DC (2014) BDNF Mediates Neuroprotection against Oxygen-Glucose Deprivation by the Cardiac Glycoside Oleandrin. J. Neurosci 4(3):963–968.

Volonte C, Ciotti MT, Merlo D (1994) LiCl promotes survival of GABAergic neurons from cerebellum and cerebral cortex: Neurosci Lett. 19;172(1-2):6-10.

Yang P, Menter DG, Cartwright C (2009) Oleandrin-mediated inhibition of human tumor cell proliferation: Importance of Na,K-ATPase a subunits as drug targets. Mol Cancer Ther. 8:2319-2328.

Ye ZC, Sontheimer H (1999) Glioma cells release excitotoxic concentrations of glutamate. Cancer Res. 59(17):4383-91.

710 **Figure legends**

711 **Figure 1 Oleandrin induces Ca^{2+} transients in human glioma cells.** (a-b) RT–PCR analyses of
712 α3 and α1 Na^+-K^+-ATPase subunit expression in tumoral, normal cells and in human tissues from
713 patients (n=3, ** p<0.01 one-way ANOVA followed by Holm Sidak post hoc test). Representative
714 experiments for some glioma cell lines are shown on top. (c) Effect of oleandrin (1 μM, 2 min) on
715 Ca^{2+} transients in U87MG cells expressed as ΔF/F0 (n = 44, ** p<0.01). (d) Proportion of U87MG
716 (black bars) and GL261 cells (white bars) displaying $[Ca^{2+}]_i$ transients in response to oleandrin (1, 3
717 and 30 μM; * p<0.05, Chi-square test). (e) Average of fluorescence responses elicited by 1, 3 and
718 30 μM oleandrin in U87MG cells (* p<0.05). Top, fluorescence traces from a representative
719 U87MG cell, showing the effect of different concentrations of oleandrin on intracellular calcium.
720
721 **Figure 2 Effects of oleandrin on human and murine glioma cells on viability and migration.**
722 (a) Growth curves of human and murine glioma cells treated with oleandrin for the indicated time
723 points. The results are expressed as percentage of untreated cells at time 0 (n=4, ** p<0.01, one-
724 way Anova followed by Dunn's post hoc). (b) Representative RT–PCR analysis of α3 and α1 Na^+-
725 K^+-ATPase subunit expression in U87MG cells transfected with α1 cDNA. (c) Growth curves of
726 U87MG cells transfected with α1 cDNA treated with oleandrin for the indicated time points (n=4
727 one-way Anova followed by Holm Sidak post hoc test). (d) Induction of apoptosis in glioma cells
728 upon oleandrin treatment (3 μM for 10 h), evaluated by flow cytometry. Data show the mean value
729 of Annexin V positive plus Annexin V/PI positive cells expressed as percentage of total cells (n=6,
730 ** p<0.01 one-way ANOVA followed by Holm Sidak post hoc test). A representative plot is shown
731 on the right for U87MG. (e) Human and murine glioma cell chemotaxis toward control medium
732 (C), CXCL12 (50 ng/ml) or EGF (100 ng/ml), in the presence or absence of oleandrin at the

indicated doses. Results are expressed as fold increase in comparison with C (n=4-5, ** p<0.01 * p<0.05, one-way Anova followed by Dunn's post hoc test).

Figure 3 Oleandrin modulates the signaling pathways activated by the chemotactic agents CXCL12 and EGF. (a,b) Analysis of pAKT in GL261 and U87MG glioma cells upon CXCL12 (50 ng/ml), EGF (100 ng/ml) and oleandrin (3 μM) stimulation (1 min). Representative experiments are shown on top of each graph. Data were normalized to total AKT and expressed as percentage of untreated cells (C). (n=4; ** p<0.01 * p<0.05 one-way ANOVA followed by Holm Sidak post hoc test). (c) GL261 and U87MG treated with CXCL12 or EGF, in the absence or presence of oleandrin (3 μM), stained with phalloidin (green), pFAK (red) and Hoechst (blue) and analyzed for pFAK mean fluorescence intensity (MFI). Representative images are shown on the left. (* p<0.05 by one-way ANOVA; n=4 followed by Holm Sidak post hoc test). Note that oleandrin also modified the actin cytoskeleton. (d) Expression of *mmp9* and *mmp2* mRNA in GL261 and U87MG treated with CXCL12 or EGF, in the absence or presence of oleandrin (3 μM), as above. Results of RT–PCR analysis are shown as fold increase versus C (n=3-5, ** p<0.01, one-way Anova on ranks).

Figure 4 Oleandrin reduces tumor size and increased mice survival. (a) Experimental scheme. Mean tumor volumes (left) and Kaplan-Meier survival curves (right) in mice bearing U87MG (b) and GL261 glioma cells (c); mean tumor volumes in mice bearing U251 (d) and GBM19 (e) glioma cells. All mice were treated with oleandrin, as indicated (n= 5-11, * p<0.05, ** p<0.01 one-way ANOVA followed by Dunn's post hoc test (b,c left); ** p<0.01 long-rank test (b,c right). Representative coronal brain sections are shown above for U87MG and GL261, at 17 days.

Figure 5 Effects of oleandrin on tumor cell proliferation and apoptosis *in vivo*. Data show the $BrdU^+$ cells in brain tumors (expressed as the mean area ± s.e.m % of the tumor) at 17 days after

U87MG (a) or GL261 (c) implantation in mice treated with oleandrin 0.3 mg/kg, as indicated (** $p<0.01$ * $p<0.05$; Student's t-test; n=4-8 mice per condition). Representative immunofluorescence images of proliferating $BrdU^+$ cells (green) under the two experimental conditions are shown on the right. The mean (± s.e.m.) area of $Casp3^+$ cells in brain tumors of mice implanted with U87MG (b) or GL261 (d) cells (** $p<0.01$; Student's t-test; n=4 mice per condition). Representative immunofluorescence images of $Casp3^+$ cells (red) are shown on the right.

Figure 6 Effect of oleandrin in the brain of mice implanted with human or murine cells. Quantification of $F4/80^+$ (a) $CD68^+$ (b) and $F4/80^+$ / $CD68^+$ (c) cells in the tumor area upon oleandrin or vehicle treatment. Graph bars represent the mean (± s.e.m.) area expressed as percentage of total tumor area. Representative immunofluorescence images are shown on the right (scale bar, 100 µm) (** $p<0.01$ * $p<0.05$ Student's t-test; n=4 mice per condition). (d) Quantification of $GFAP^+$ cells at the border of tumor mass (mean ± s.e.m. of area of as % of the tumor area, * $p<0.05$, Student's t-test, n=4 mice per condition) 17 days after U87MG or GL261 transplantation in mice treated with vehicle or oleandrin, as indicated. Representative immunofluorescence images are shown on the right. (e) Mean number (± s.e.m.) of different human and murine glioma cells invading the brain parenchyma for more than 150 µm (n=3-5 mice per condition; ** $p<0.01$ Student's t-test). Right: representative coronal brain sections stained with hematoxylin/eosin. Black arrows indicate invading glioma cells beyond the main tumor border (dashed line). For all the panels: scale bars, 10 µm.

Figure 7 Oleandrin induces BDNF expression. Expression of *bdnf* mRNA (a,c) and protein (b,d) in contra- (C) and ipsilateral (I) hemispheres of GL261- or U87MG-bearing mice treated with oleandrin 0.3 mg/kg, as indicated. Results of real time–PCR analysis are shown as fold increases with respect to C (n=5-4, * $p<0.05$, ** $p<0.01$ one-way ANOVA followed by Dunn's post hoc test).

(e) Expression of *bdnf* (mRNA) in $NeuN^+$ cells isolated from contra- and ipsilateral hemispheres of GL261-bearing mice treated with vehicle or oleandrin. Results are shown as fold increases (*vs* C) (n=5, one-way ANOVA followed by Tukey post hoc test; * $p<0.05$ ** $p<0.01$). (f) Effect of 3 μM oleandrin (the bar refers to 2 min) on Ca^{2+} transients in cortical neurons, expressed as ΔF/F0 (n = 15, **$p<0.01$, Chi-square test). (g) Mean tumor volumes (GL261 and shRNA-TrkB GL261) in *wt* (C57BL/6) and/or $bdnf^{+/-}$ mice, treated with oleandrin (0.3 mg/kg), as indicated (n=5, * $p<0.05$ one-way ANOVA followed by Holm Sidak post hoc test). Representative coronal brain sections are shown above for *wt* and $bdnf^{+/-}$ mice (at 17 days).

Figure 8 TrkB isoform expression and effect of BDNF on human glioma cell chemotaxis. (a) RT–PCR analyses of TrkB isoform expression in U87MG, U251, GBM19 and normal human cerebral tissue as control. (b) Glioma cell chemotaxis toward BDNF (100 ng/ml) and/or EGF (100 ng/ml). Chemotaxis is expressed as fold increase with respect to C (n=5; ** $p<0.01$ one-way Anova).

Figure 9 Oleandrin increases TMZ-induced mice survival. Kaplan-Meier survival curves of GL261 glioma bearing mice treated with vehicle, oleandrin (0.3 mg/kg), TMZ (50 mg/kg) or both (Ole + TMZ) (n=9-11, ** $p<0.01$ vs C; ## $p<0.01$ vs TMZ and Ole log rank test).

Figure 10 Schematic oleandrin effects on glioma. Oleandrin has direct effects on human GBM, reducing viability. It also stimulates neurons to release BDNF, that impairs tumor cell chemotaxis, and modulates tumor microenvironment. All these effects contribute to reduce glioma growth in mouse brain. See discussion for details.

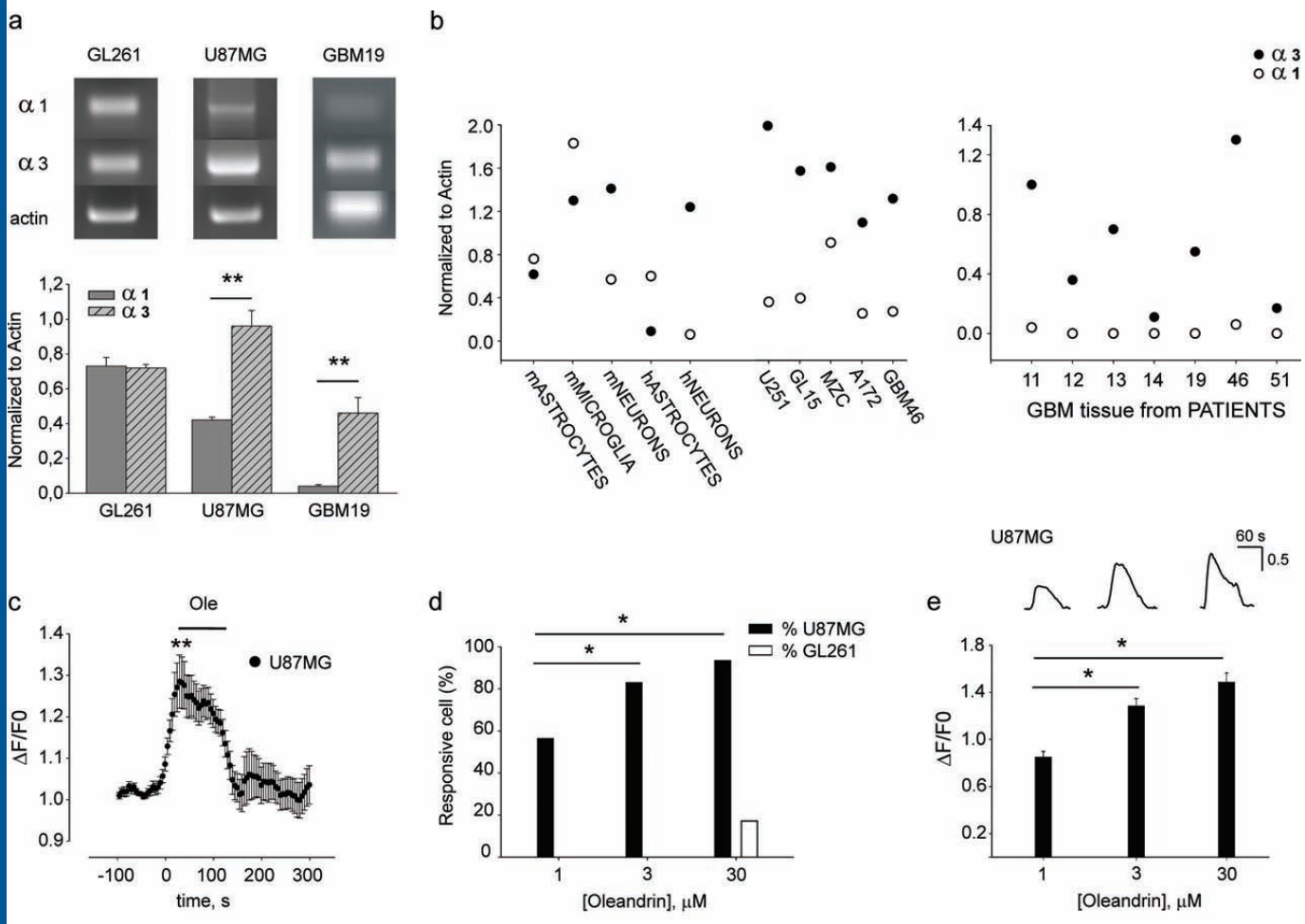

Garofalo et al. Fig. 1

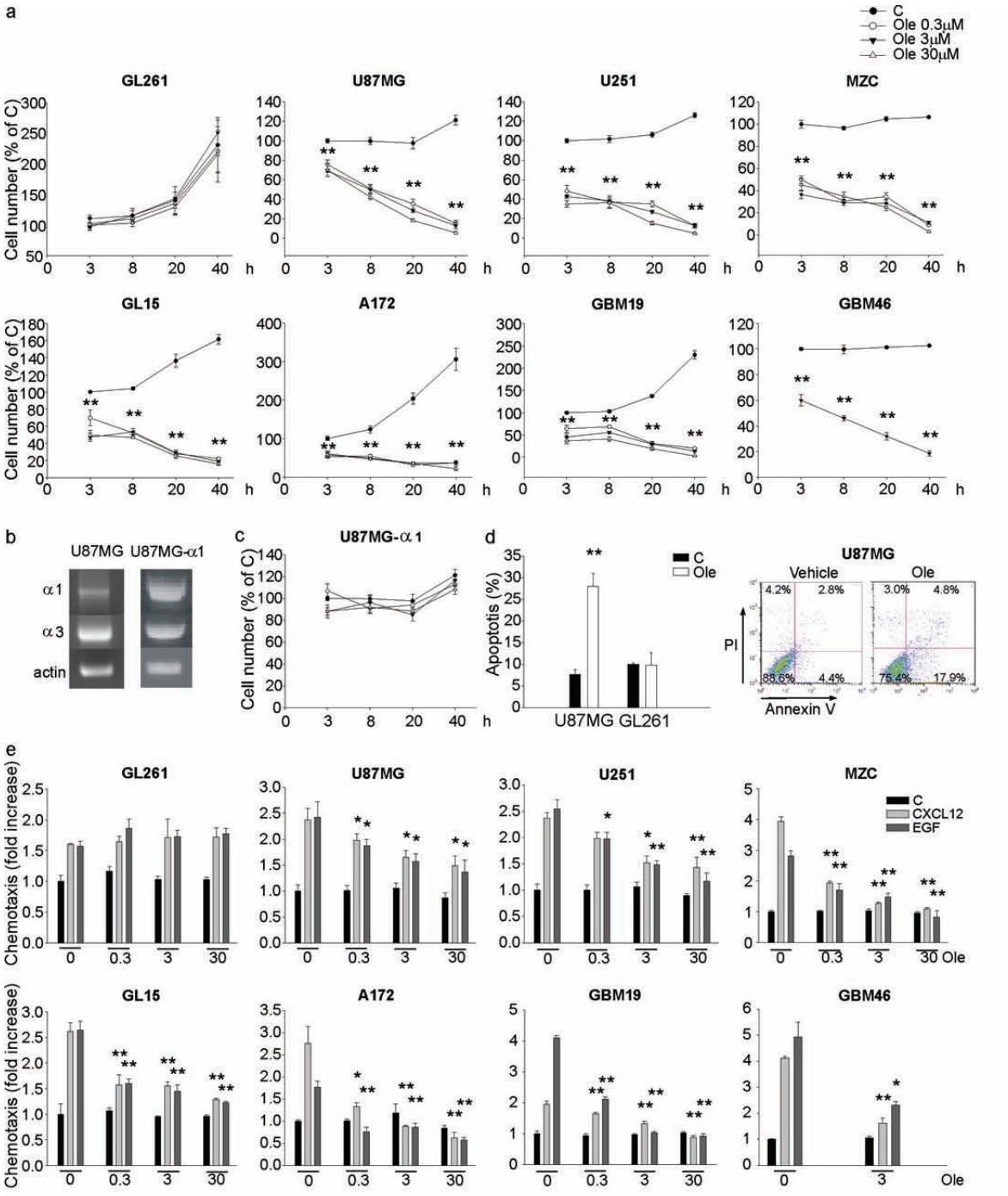

Garofalo et al. Fig. 2

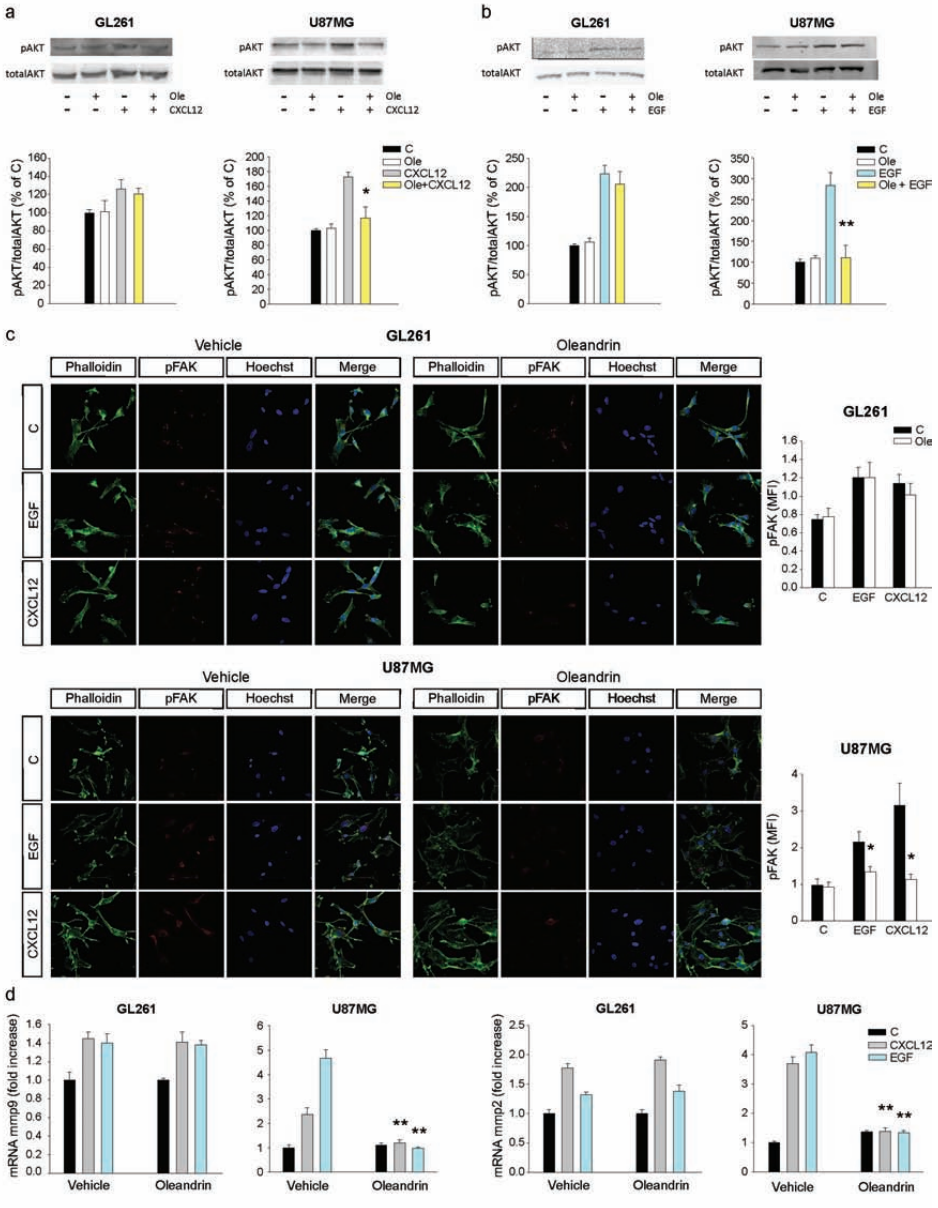

Garofalo et al. Fig. 3

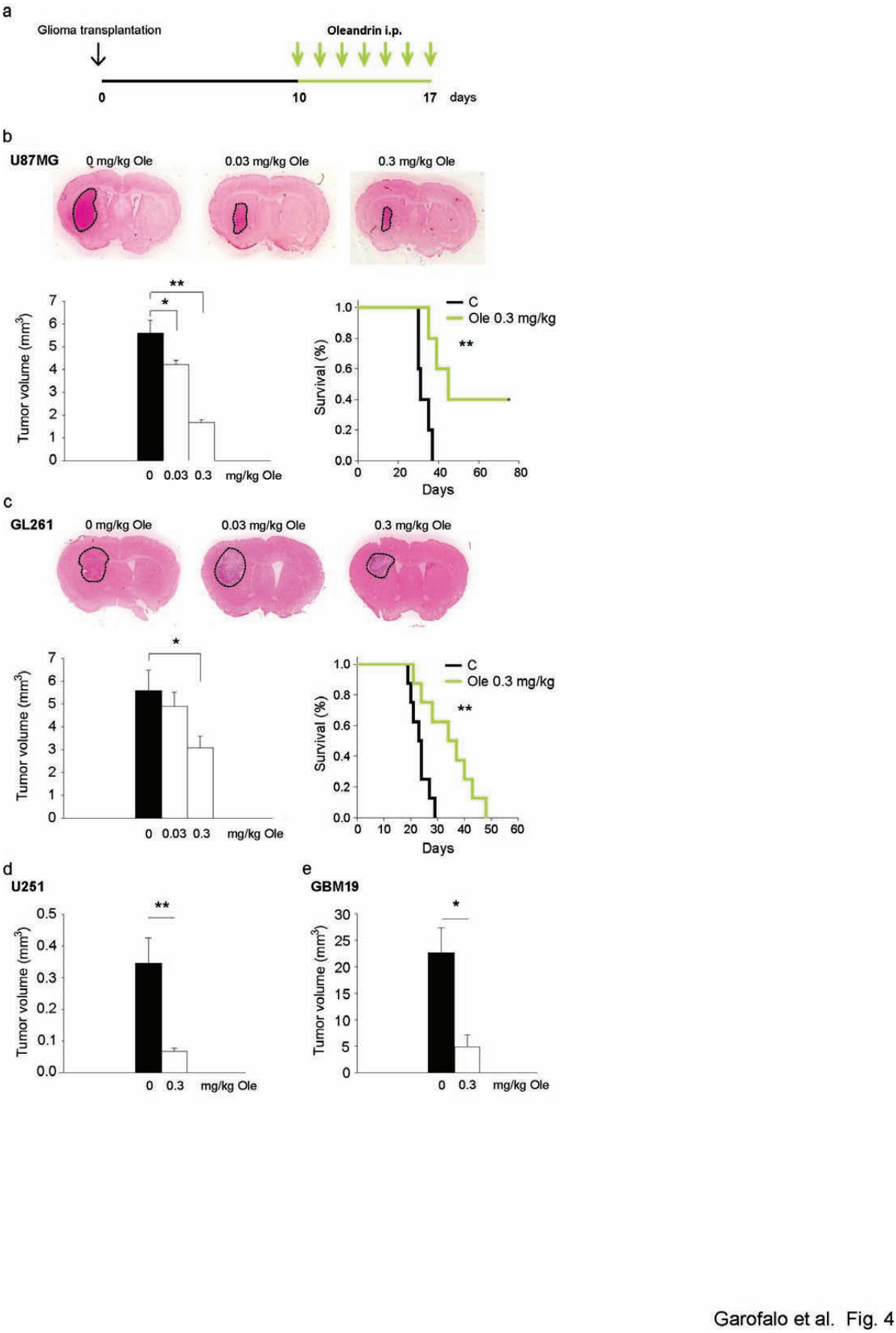

Garofalo et al. Fig. 4

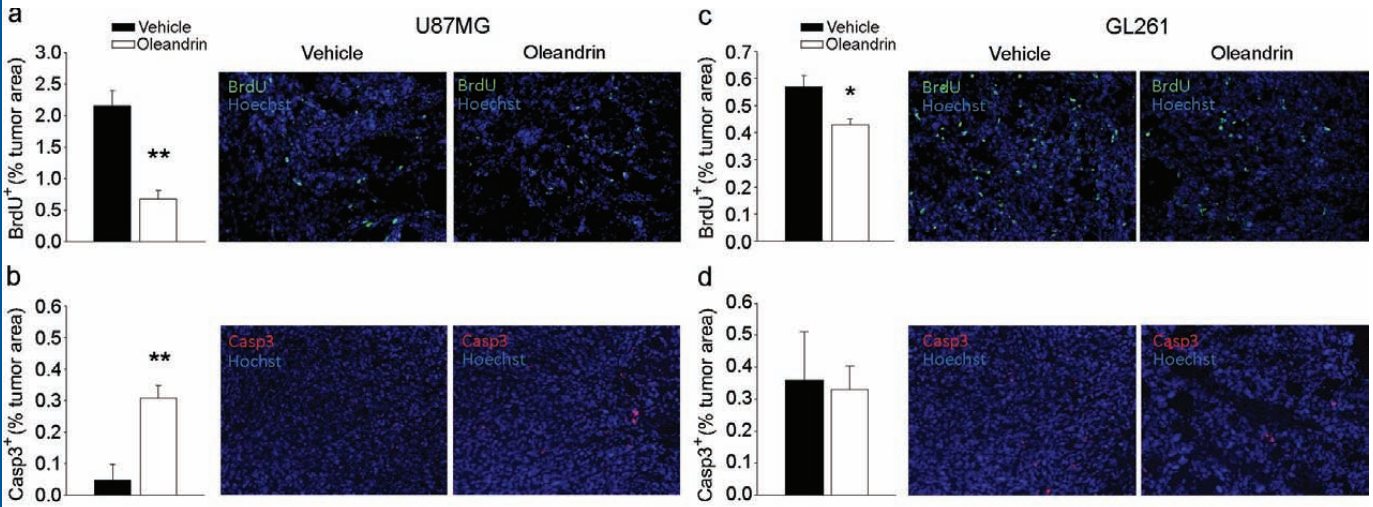

Garofalo et al. Fig. 5

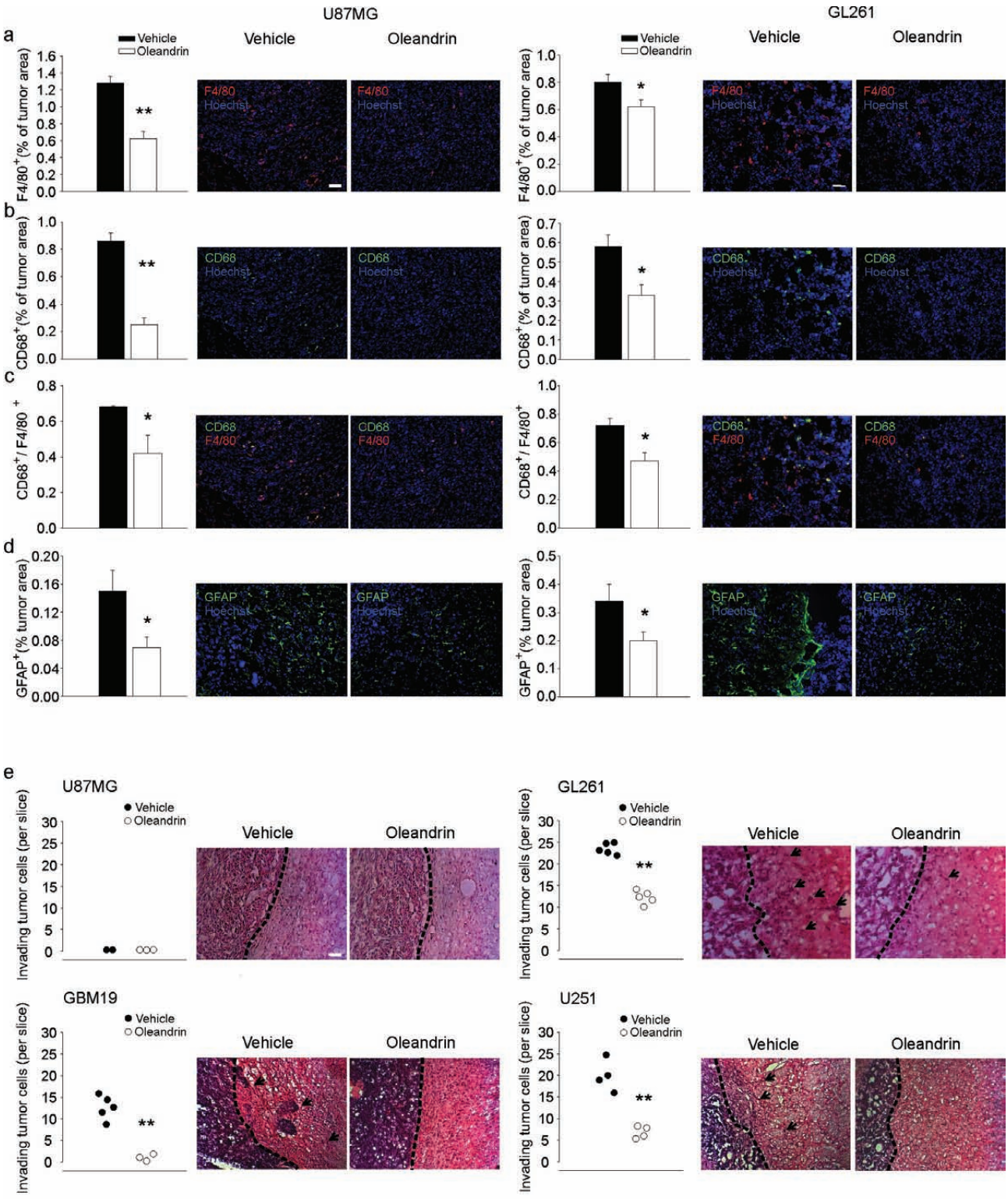

Garofalo et al. Fig. 6

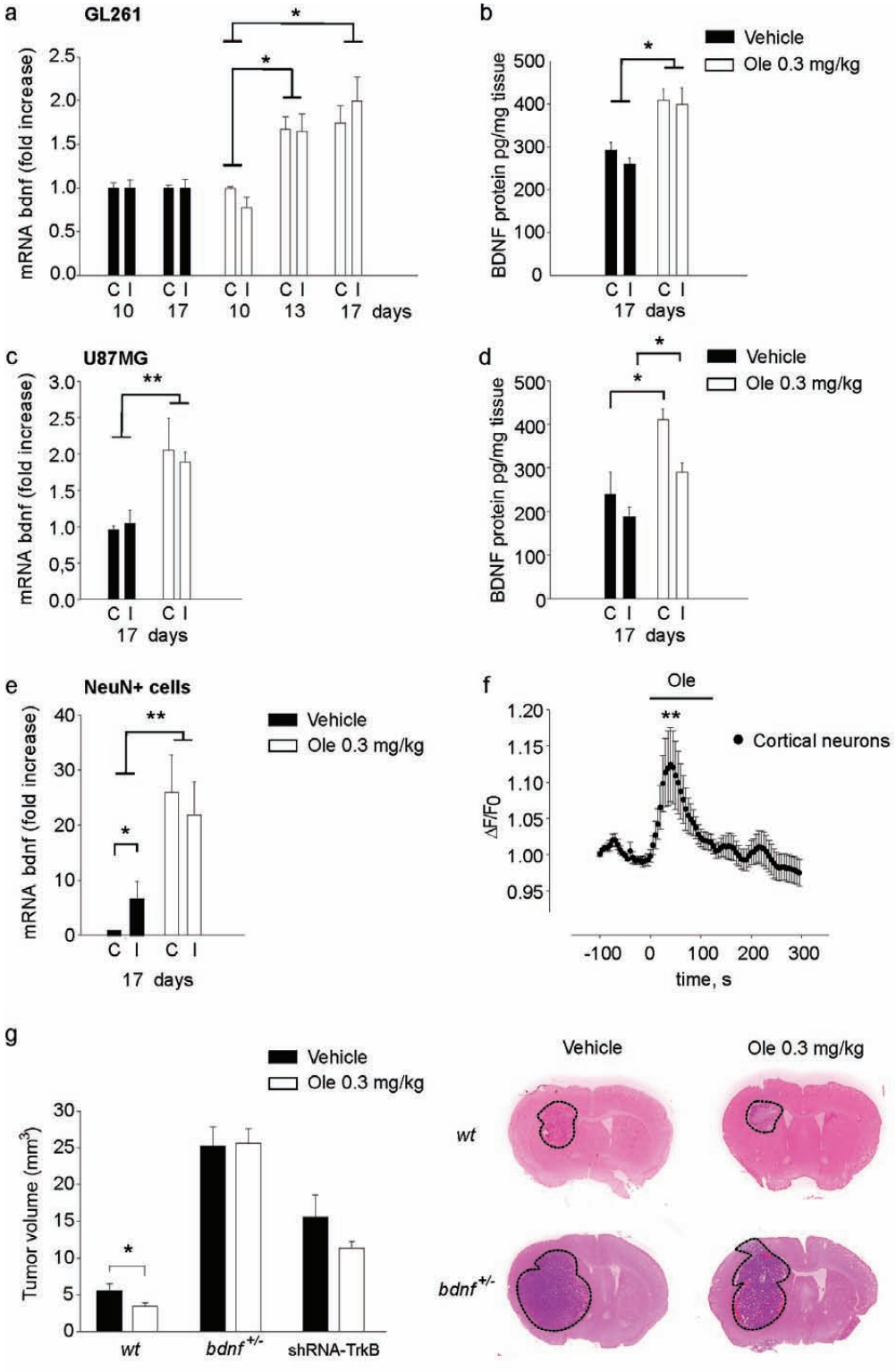

Garofalo et al. Fig. 7

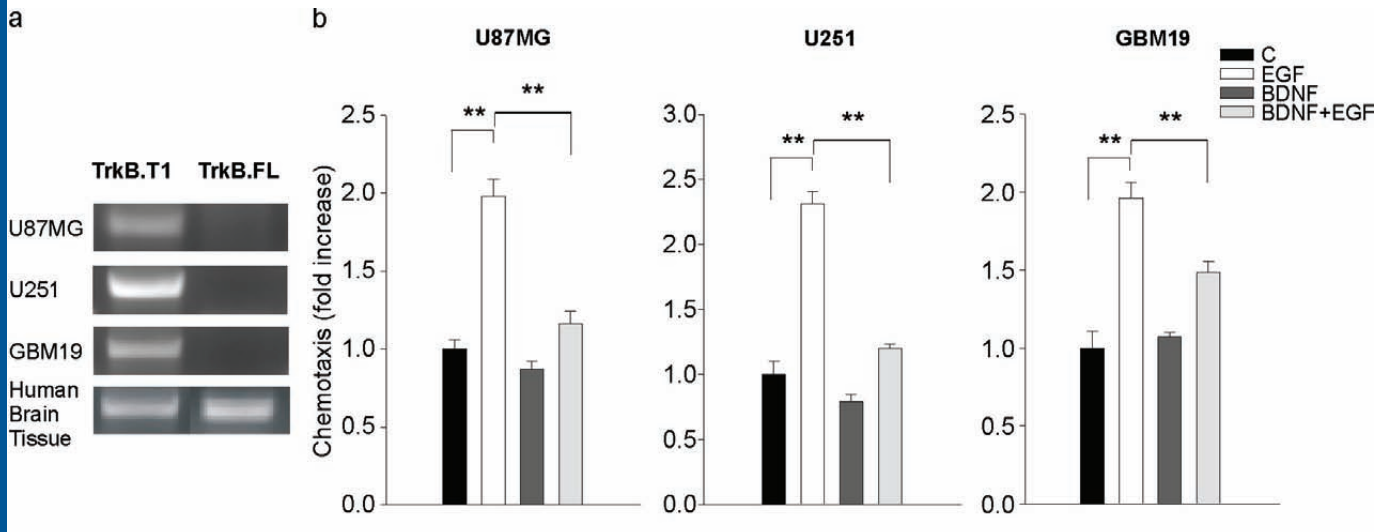

Garofalo et al. Fig. 8

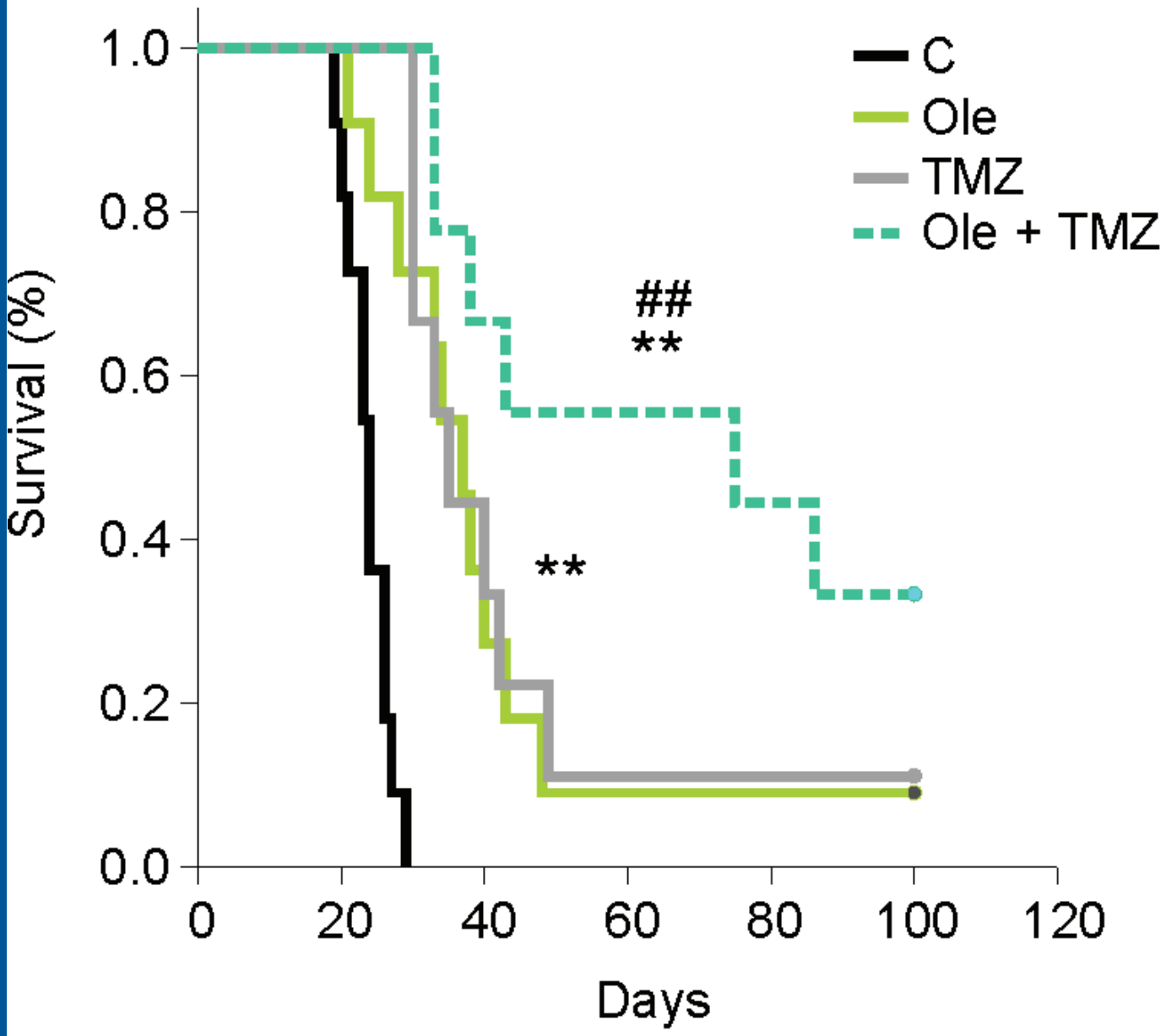

Garofalo et al. Fig. 9

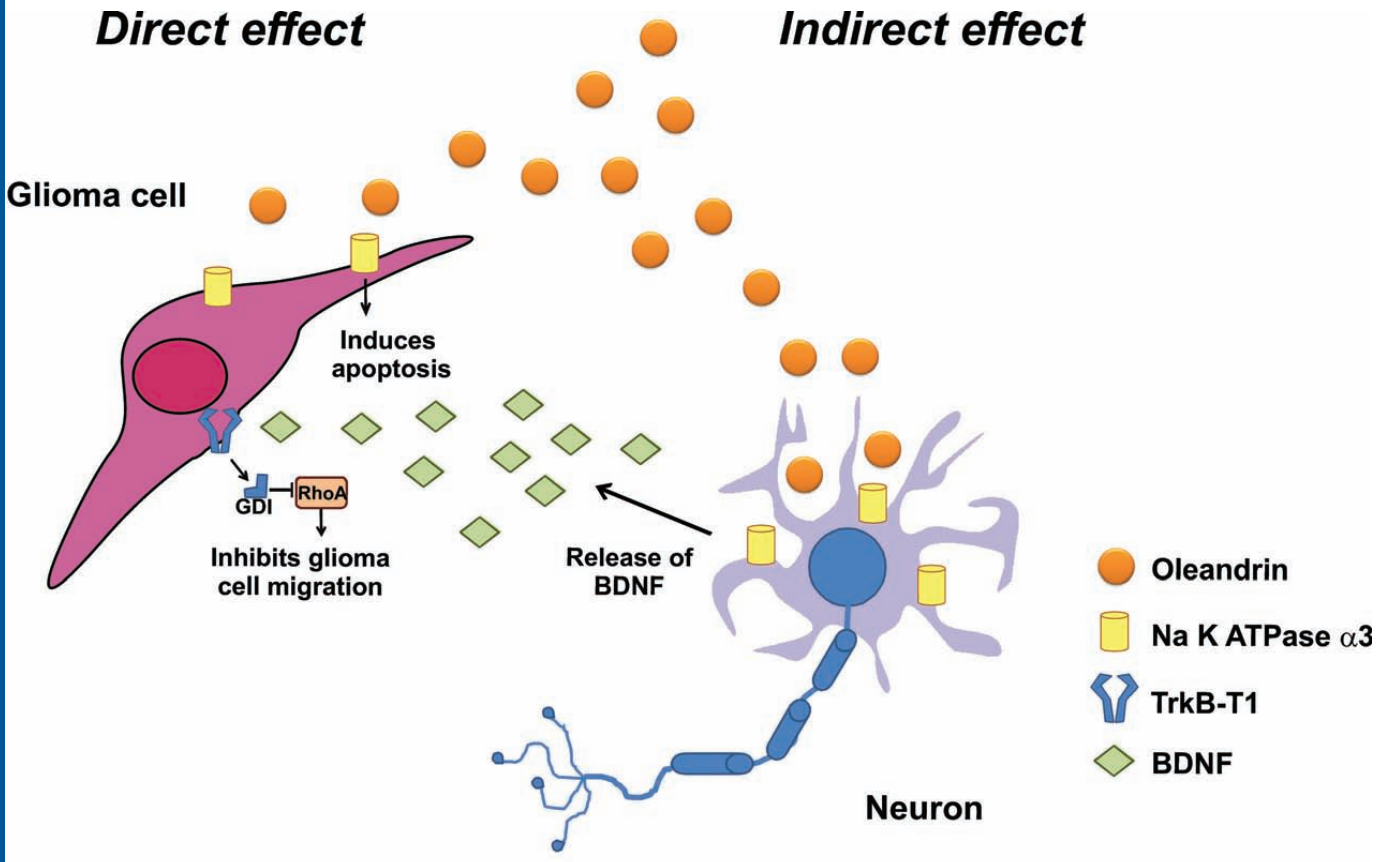

Garofalo et al. Fig.10